

AN INNOVATIVE COMPUTATIONAL METHOD FOR PREDICTING NEUTRON TRANSPORT

Approved for public release; distribution is unlimited.

March 2000



Prepared for:
Defense Threat Reduction Agency
45045 Aviation Drive
Dulles, VA 20166-7517

DNA001-96-C-0103

Jay I. Frankel

Prepared by: University of Tennessee - Knoxville
College of Engineering
414 Dougherty Engineering Building
Knoxville, TN 37996-2210

20000828 006

DESTRUCTION NOTICE:

Destroy this report when it is no longer needed. Do not return to sender.

PLEASE NOTIFY THE DEFENSE THREAT REDUCTION AGENCY, ATTN: ADM, 6801 TELEGRAPH ROAD, ALEXANDRIA, VA. IF YOUR ADDRESS IS INCORRECT, IF YOU WISH IT DELETED FROM THE DISTRIBUTION LIST, OR IF THE ADDRESSEE IS NO LONGER EMPLOYED BY YOUR ORGANIZATION.

DISTRIBUTION LIST UPDATE

This mailer is provided to enable DTRA to maintain current distribution lists for reports. (We would appreciate you providing the requested information.)

- ☐ Add the individual listed to your distribution list.
- ☐ Delete the cited organization/individual.
- ☐ Change of address.

Note:

Please return the mailing label from the document so that any additions, changes, corrections or deletions can be made easily. For distribution cancellation or more information call DTRA/ADM (703) 325-1036.

NAME: _____

ORGANIZATION: _____

OLD ADDRESS

NEW ADDRESS

TELEPHONE NUMBER: () _____

DTRA PUBLICATION NUMBER/TITLE

CHANGES/DELETIONS/ADDITIONS, etc.)

(Attach Sheet if more Space is Required)

DTRA or other GOVERNMENT CONTRACT NUMBER: _____

CERTIFICATION of NEED-TO-KNOW BY GOVERNMENT SPONSOR (if other than DTRA):

SPONSORING ORGANIZATION: _____

CONTRACTING OFFICER or REPRESENTATIVE: _____

SIGNATURE: _____

CUT HERE AND RETURN

DEFENSE THREAT REDUCTION AGENCY
ATTN: ADM
45045 AVIATION DRIVE
DULLES, VA 20166-7517

DEFENSE THREAT REDUCTION AGENCY
ATTN: ADM
6801 TELEGRAPH ROAD
ALEXANDRIA, VA 22310-3398

REPORT DOCUMENTATION PAGE			Form Approved OMB No. 0704-0188	
<small>Public reporting burden for this collection of information is estimated to average 1 hour per response, including the time for reviewing instructions, searching existing data sources, gathering and maintaining the data needed, and completing and reviewing the collection of information. Send comments regarding this burden estimate or any other aspect of this collection of information, including suggestions for reducing this burden, to Washington Headquarters Services, Directorate for Information Operations and Reports, 1215 Jefferson Davis Highway, Suite 1204, Arlington, VA 22202-4302, and to the Office of Management and Budget, Paperwork Reduction Project (0704-0188), Washington, DC 20503</small>				
1. AGENCY USE ONLY (Leave blank)	2. REPORT DATE March 2000	3. REPORT TYPE AND DATES COVERED Technical 960623-980622		
4. TITLE AND SUBTITLE An Innovative Computational Method for Predicting Neutron Transport		5. FUNDING NUMBERS C -DNA 001-96-C-0103 PE -62715H PR -AF TA -D WU -DH53052		
6. AUTHOR(S) Jay I. Frankel				
7. PERFORMING ORGANIZATION NAME(S) AND ADDRESS(ES) University of Tennessee-Knoxville College of Engineering 414 Dougherty Engineering Building Knoxville, Tennessee 37996-2210		8. PERFORMING ORGANIZATION REPORT NUMBER		
9. SPONSORING/MONITORING AGENCY NAME(S) AND ADDRESS(ES) Defense Threat Reduction Agency 45045 Aviation Drive Dulles, VA 20166-7517 CPWP/Kehlet		10. SPONSORING MONITORING AGENCY REPORT NUMBER DSWA-TR-98-62		
11. SUPPLEMENTARY NOTES This work was sponsored by the Defense Threat Reduction Agency under RDT&E RMC code B 4662 D AD 53052 3200 A AF 25904D.				
12a. DISTRIBUTION/AVAILABILITY STATEMENT Approved for public release; distribution is unlimited.		12b. DISTRIBUTION CODE		
13. ABSTRACT (Maximum 200 words) This final report indicates the work performed under DNA-001-96-0103 during the span covering June 1996 through June 1998. Several important findings are reported strongly suggesting that the proposed numerical methodology can perform as initially conceived upon resolving the remaining technical issue involving the numerical integration of integral containing Hadamard type kernels. Preliminary calculations are presented in both cartesian and spherical geometries indicating that the symbolically augmented method has merit when addressing the numerical simulation of the integral form of the linearized Boltzmann transport equation.				
14. SUBJECT TERMS Symbolic manipulation, Fredholm integral equations, singular kernels, Linearized transport equation		15. NUMBER OF PAGES 56		
		16. PRICE CODE		
17. SECURITY CLASSIFICATION OF REPORT UNCLASSIFIED	18. SECURITY CLASSIFICATION OF THIS PAGE UNCLASSIFIED	19. SECURITY CLASSIFICATION OF ABSTRACT UNCLASSIFIED	20. LIMITATION OF ABSTRACT SAR	

Table of Contents

Section	Page
Figures	iii
Tables	iv
1 Summary.....	1
2 Concept Development.....	2
2.1 Introduction.....	2
2.2 Symbolic Form of the Kernels.....	2
2.3 Orthogonal Collocation with Chebyshev Basis (Isotropic Scattering Case).....	4
2.4 Orthogonal Collocation with Chebyshev Basis (Linear Anisotropic Case).....	7
2.5 Orthogonal Collocation with Chebyshev Basis (Anisotropic Case [12]).....	10
3 Symbolic Manipulation of the Kernel Functions	19
3.1 Identification of the Kernel in Terms of Known Functions	19
3.2 General Anisotropic Scattering Cases	19
3.3 Identification of $K_{m,n}(\eta, \xi)$ in Terms of Known Functions.....	20
3.4 Modified Kernel Approach.....	22
3.5 Identified Anisotropic Scattering Test Phase Function	23
4 Conclusions and Recommendations.....	25
5 References.....	26
 Appendix	
DAHC35-95-P-3171 [4]	A-1

Figures

Figure	Page
1 $\Phi_0(\eta)$ and $\Phi_1(\eta)$ distributions for various values of N when $\omega = 0.5$, $a_1 = -2.7$ and $R = 1$	17
2 $\Phi_0(\eta)$ and $\Phi_1(\eta)$ distributions for various values of N when $\omega = 0.5$, $a_1 = -2.7$ and $R = 5$	18
3 Simple back-scattering phase function.....	24
4 Highly lobular phase function.....	24

Tables

Table		Page
1	Numerical results for the reflectivity using the proposed Chebyshev collocation method for various ω and R	7
2	Comparison of results for the emissivity, ϵ using the proposed method with that of a Galerkin solution [12] when $R = 1$ for various ω and N	13
3	Comparison of results for the emissivity, ϵ using the proposed method with that of a Galerkin solution [12] when $R = 5$ for various ω and N	14
4	Expansion coefficients for $\Phi_0(\eta)$ when $R = 1$, $a_1 = -2.7$, and $\omega = 0.5$	14
5	Expansion coefficients for $\Phi_1(\eta)$ when $R = 1$, $a_1 = -2.7$, and $\omega = 0.5$	15
6	Expansion coefficients for $\Phi_0(\eta)$ when $R = 5$, $a_1 = -2.7$, and $\omega = 0.5$	15
7	Expansion coefficients for $\Phi_1(\eta)$ when $R = 5$, $a_1 = -2.7$, and $\omega = 0.5$	16

Section 1

Summary

This final report indicates the work performed under DNA-001-96-0103 during the span covering June 1996 through June 1998. Several important findings are reported strongly suggesting that the proposed numerical methodology can perform as initially conceived upon resolving the remaining technical issue involving the numerical integration of integral containing Hadamard type kernels. Preliminary calculations are presented in both cartesian and spherical geometries indicating that the symbolically augmented method has merit when addressing the numerical simulation of the integral form of the linearized Boltzmann transport equation.

Section 2

Concept Development

2.1 Introduction.

In a series of articles [1-3], a symbolically enhanced methodology has been developed for solving the integral form of the Boltzmann transport equation in the presence of anisotropy. The integral for the transport equation has been utilized in these past one-dimensional studies since a reduction in dimensionality occurs. The resulting system of weakly singular Fredholm integral equations of the second kind involves the various Legendre moments of intensity (radiative transport) or neutron flux (neutron transport).

In [1], an important computational attribute was reported. It was observed that symbolic could be used to automate the identification of the kernel function needed to arrive at the integral form of the transport equation in a slab geometry. Theoretical considerations involving convergence and error analyses were established [2,3] based on a weighted residual methodology where Chebyshev polynomials were used as the basis set in the series expansion of the unknown dependent variables. The convergence rate was established for the isotropic scattering case when implementing orthogonal collocation. In [3], LaClair and Frankel investigated linear anisotropic scattering and developed rigorous error estimates based on functional analysis that extended the error estimates developed in [2].

This report focuses on the spherical coordinate problem and extends the numerical findings reported in [4] which involved highly anisotropic scattering in a plane-parallel geometry. This singular geometry produces additional analytical and numerical difficulties that do not appear in the plane-parallel geometry associated with a one-dimensional slab geometry. Attention is first directed toward the identification of a method for symbolically representing the kernel function in the spherical coordinate system. Finally, some discussion is directed toward developing a numerical solution to a series of coupled integral equations containing these newly formed kernel functions.

The first two-thirds of the research effort was highly successful. The final one-third, which involved numerical integration of singular integrand, was not as successful. If the program would to continue for an additional year, this final hurdle should be resolvable.

2.2 Symbolic Form for the Kernels.

Unlike Phase I of this investigation, which involved the integral form linearized Boltzmann transport equation in a plane-parallel geometry, symbolic implementation in the spherical geometry is not as straightforward. This was seen during July 1996. Fortunately, an observation was made making use of a new intermediate form which allows for the symbolic implementation to be accomplished. This observation does not follow conventional expressions used in describing the kernel functions.

As noted by Thynell and Ozisik [5], the necessary kernel for the integral form of the transport equation in the spherical coordinate system is

$$K_{mn}(r, x) = \int_{t=|r-x|}^{r+x} P_m\left(\frac{r^2 - x^2 - t^2}{2xt}\right) P_n\left(\frac{r^2 - x^2 + t^2}{2rt}\right) \frac{e^{-t}}{t} dt, \quad m, n = 0, 1, \dots, N, \quad (1)$$

where $P_m(u)$ represents the m^{th} Legendre polynomial of the first kind. Letting $y = r + x$ and $z = |r - x|$ allows Eq. (1) to be given as

$$K_{mn}(r, x) = \int_{t=z}^y P_m\left(\frac{r^2 - x^2 - t^2}{2xt}\right) P_n\left(\frac{r^2 - x^2 + t^2}{2rt}\right) \frac{e^{-t}}{t} dt, \quad m, n = 0, 1, \dots, N. \quad (2)$$

Unlike the slab geometry [4], some additional algebraic effort and some new function definitions must be introduced in order to arrive at a form conducive to symbolic manipulation. For illustrative purposes, we shall consider the case where $m = n = 1$, therefore our attention is focused on

$$K_{11}(r, x) = \int_{t=z}^y P_1\left(\frac{r^2 - x^2 - t^2}{2xt}\right) P_1\left(\frac{r^2 - x^2 + t^2}{2rt}\right) \frac{e^{-t}}{t} dt, \quad m, n = 0, 1, \dots, N, \quad (3)$$

where $P_1(u) = u$. Expanding the polynomial product of the Legendre polynomials of the first kind and then simplifying and collecting terms produces

$$K_{11}(r, x) = -\frac{1}{4rx} \int_{t=z}^y te^{-t} dt + \frac{(x^2 - r^2)^2}{4rx} \int_{t=z}^y \frac{e^{-t}}{t^3} dt. \quad (4)$$

Let

$$G_3(y, z) = \int_{t=z}^y \frac{e^{-t}}{t^3} dt, \quad (5)$$

therefore

$$K_{11}(r, x) = -\frac{1}{4rx} \int_{t=z}^y te^{-t} dt + \frac{(x^2 - r^2)^2}{4rx} G_3(y, z). \quad (6)$$

In general, we can define

$$G_j(y, z) = \int_{t=z}^y \frac{e^{-t}}{t^j} dt, \quad j = 0, 1, \dots, \quad (7)$$

and use this definition in developing a general expression for the kernel function. Using Eq. (7), the integral can be analytically evaluated to

$$G_j(y, z) = \frac{1}{z^{j-1}} E_j(z) - \frac{1}{y^{j-1}} E_j(y), \quad j = 0, 1, \dots \quad (8)$$

This definition for $G_j(y, z)$ can be used to describe any degree of anisotropy. For example,

$$K_{00}(r, x) = G_1(y, z), \quad (9)$$

$$K_{01}(r, x) = \frac{r^2 - x^2}{2r} G_2(y, z) + \frac{1}{2r} \int_{t=z}^y e^{-t} dt, \quad (10)$$

$$K_{10}(r, x) = \frac{r^2 - x^2}{2x} G_2(y, z) - \frac{1}{2x} \int_{t=z}^y e^{-t} dt, \quad (11)$$

$$K_{11}(r, x) = \frac{(r^2 - x^2)^2}{4rx} G_3(y, z) - \frac{1}{4rx} \int_{t=z}^y te^{-t} dt, \quad (12)$$

where $y = r + x$ and $z = |r - x|$. Also, the remaining integrals displayed in Eqs. (10-12) can clearly be integrated analytically.

This procedure can continue, though as m and n increase, the algebraic level of difficulty also increases. The functions described in Eqs. (9-12) have been verified using the study performed by Abulwafa [6].

2.3 Orthogonal Collocation with Chebyshev Basis (Isotropic Scattering Case).

A preliminary simulation was performed to indicate the accuracy, relative speed, and memory requirements for the one-speed, bare sphere, isotropic scattering albedo problem [2,5,6-10]. This problem is well-studied and the open literature offers benchmark numerical results as obtained by the F-N method [8] and by the Galerkin method with a nonorthogonal basis set [7]. These results report the numerical value for the albedo for various scattering coefficients and radii. Also, both [8] and [7] report the number of terms necessary in the series representation to obtain five digit accuracy for the albedo. It should be noted that the calculation of the albedo requires fewer terms to achieve five digit accuracy than the actual neutron flux. This occurs because of the integral definition of the albedo in terms of the zeroth Legendre moment of the neutron flux.

In order to verify and evaluate the accuracy of the approach, preliminary calculations are developed using the radiative heat transfer community results. Tabular results have been reported by Ozisik and his co-workers over the last decade.

Defining the m^{th} Legendre moment of the intensity, $I(r, \mu)$ as

$$G_m(r) = 2\pi \int_{\mu=-1}^1 P_m(\mu) I(r, \mu) d\mu, \quad m = 0, 1, \dots, N, \quad (13)$$

where $P_m(z)$ represents the m^{th} Legendre polynomial of the first kind. With this definition, the linearized Boltzmann transport equation can be expressed in an integral form. Following Thynell and Ozisik [5], the general integral form of the transport equation in spherical coordinates can be expressed as

$$\begin{aligned} rG_n(r) = 2\pi \int_{x=0}^R \left[Q(x)K_{0n}(r, x) + \frac{\omega}{4\pi} \sum_{m=0}^N b_m G_m(x) K_{mn}(r, x) \right] x dx + \\ 2\pi r \int_{\mu=0}^1 [(-1)^n e^{r\mu} + e^{-r\mu}] I^-[R, -\mu_o(r, \mu)] P_n(\mu) e^{-\alpha(R, r, \mu)} d\mu, \\ x \in [0, R], \quad n = 0, 1, \dots, N, \end{aligned} \quad (14)$$

where the kernel function $K_{mn}(r, x)$ is given by

$$K_{mn}(r, x) = \int_{t=|r-x|}^{r+x} P_m\left(\frac{r^2 - x^2 - t^2}{2xt}\right) P_n\left(\frac{r^2 - x^2 + t^2}{2rt}\right) \frac{e^{-t}}{t} dt, \quad m, n = 0, 1, \dots, N, \quad (15)$$

while

$$\alpha(x, r, \mu) = \sqrt{x^2 - r^2(1 - \mu^2)}, \quad (16)$$

and

$$\mu_o(r, \mu) = \sqrt{1 - (r/R)^2(1 - \mu^2)}, \quad (17)$$

Assuming a transparent boundary at $r = R$ allows us to write the boundary condition [7]

$$I^-(R, -\mu) = f(\mu), \quad \mu > 0. \quad (18)$$

In deriving Eq. (17), the conventional form of the phase function was assumed; namely,

$$p(\mu, \mu') = \sum_{m=0}^N b_m P_m(\mu) P_m(\mu'), \quad b_0 = 1, \quad (19)$$

where the $\{b_m\}_{m=0}^N$ are known coefficients.

In the case of isotropic scatter ($N = 0$), the kernel displayed in Eq. (15) reduces to

$$K_{00}(r, x) = E_1(|r - x|) - E_1(r + x), \quad x, r \in [0, R], \quad (20)$$

where $E_1(z)$ represents the first exponential integral function which contains a known logarithmic singularity as $z \rightarrow 0$.

In order to introduce the Chebyshev basis functions later, we need map the domain from $r \in [0, R]$ to $\eta \in [-1, 1]$. Clearly,

$$r = \lambda(1 + \eta), \quad r \in [0, R], \quad \eta \in [-1, 1], \quad (21)$$

where $\lambda = R/2$ accomplishes the required transformation. Using Eq. (21), the transport equation shown in Eq. (14) can be written as

$$\lambda(1 + \eta)\Psi(\eta) = \lambda(1 + \eta)F(\eta) + \frac{\omega\lambda^2}{2} \int_{\xi=-1}^1 (1 + \xi)\Psi(\xi)k_{00}(\eta, \xi)d\xi, \quad \eta \in [-1, 1], \quad (22)$$

where

$$\Psi(\eta) = G_0(\lambda(1 + \eta)), \quad (23)$$

$$k_{00}(\eta, \xi) = K_{00}(\lambda(1 + \eta), \lambda(1 + \xi)) = E_1(\lambda|\eta - \xi|) - E_1(\lambda(2 + \eta + \xi)), \quad (24)$$

while

$$F(\eta) = 4\pi \int_{\mu=0}^1 \cosh[\lambda(1 + \eta)\mu] e^{-\sqrt{R^2 - \lambda^2(1 + \eta)^2(1 - \mu^2)}} d\mu, \quad \eta \in [-1, 1], \quad (25)$$

where $f(\mu) = 1$, i.e., isotropically incident source at $r = R$.

Let the solution for $\Psi(\eta)$ be expressible in terms of an infinite series; namely,

$$\Psi(\eta) = \sum_{j=0}^{\infty} a_j T_j(\eta), \quad \eta \in [-1, 1], \quad (26)$$

where $\{T_j(\eta)\}_{j=0}^{\infty}$ represent Chebyshev polynomials of the first kind. The unknown expansion coefficients are denoted by the infinite set of constants $\{a_j\}_{j=0}^{\infty}$. In practice, this infinite series representation must be truncated after a finite number of terms, say, $N + 1$. Therefore, we form an approximation to $\Psi(\eta)$ which is denoted as $\Psi_N(\eta)$ and is given by

$$\Psi(\eta) \approx \Psi_N(\eta) = \sum_{j=0}^N a_j^N T_j(\eta), \quad \eta \in [-1, 1]. \quad (27)$$

Upon substituting the assume expansion for the unknown function $\Psi_N(\eta)$ into Eq. (22), the residual equation is formed; namely,

$$R_N(\Psi_N(\eta)) = \lambda(1 + \eta)F(\eta) - \sum_{j=0}^N a_j^N [\lambda(1 + \eta)T_j(\eta) - \frac{\omega\lambda^2}{2}A_j(\eta)], \quad \eta \in [-1, 1], \quad (28)$$

where

$$A_j(\eta) = \int_{\xi=-1}^1 (1 + \xi)T_j(\xi)k_{00}(\eta, \xi)d\xi, \quad j = 0, 1, \dots, N, \quad \eta \in [-1, 1]. \quad (29)$$

The function defined in Eq. (29) can be integrated analytically without difficulty. Numerical evaluation of the weakly singular integrand can also be accomplished by first performing one or more integration by parts prior to applying a numerical quadrature.

For illustration and comparison purposes, we propose to use orthogonal collocation. Unlike the Galerkin method, this method does not require any additional integrations to be performed. The collocation method is defined through the following inner product (orthogonality) statement

$$\left\langle R_N(\Psi_N(\eta)), \delta(\eta - \eta_k) \right\rangle_1 = 0, \quad k = 0, 1, \dots, N. \quad (30)$$

Here, the collocation points are denoted as η_k , $k = 0, 1, \dots, N$ and given by the open rule

$$\eta_k = \cos \left[\frac{(2k + 1)\pi}{2(N + 1)} \right], \quad k = 0, 1, \dots, N. \quad (31)$$

Substituting Eq. (28) into Eq. (30) produces a system of linear equations for the unknown expansion coefficients; namely,

$$\sum_{j=0}^N a_j^N [\lambda(1 + \eta_k)T_j(\eta_k) - \frac{\omega\lambda^2}{2}A_j(\eta_k)] = \lambda(1 + \eta_k)F(\eta_k), \quad k = 0, 1, \dots, N. \quad (32)$$

This linear system can solved by conventional means without difficulty. For sake of comparison with the published results of Thynell and Ozisik [7], we need to introduce the property of reflectivity. Here, the reflectivity is defined as

$$Ref = 2\pi \int_{\mu=0}^1 \mu e^{-2\mu R} d\mu +$$

$$\frac{\omega\lambda^3}{R^2} \int_{\eta=-1}^1 (1+\eta)^2 \Psi(\eta) \int_{t=0}^1 \cosh[\lambda(1+\eta)t] e^{-\sqrt{R^2-\lambda^2(1+\eta)^2(1-\mu^2)}} dt d\eta. \quad (33)$$

To illustrate the effectiveness of orthogonal collocation, Table 1 presents a suite of results for the reflectivity as defined by Eq. (33). The results presented in Table 1 use various values of ω and radii (R). These simulations are compared to the results of Thynell and Ozisik [7]. Thynell and Ozisik [7] developed benchmark results using a Galerkin method. The last column in Table 1 indicates their results and the number of terms required to obtain five digit accuracy in the reflectivity calculation. It is clear from viewing this table, that the proposed Chebyshev collocation method produces benchmark accuracy. Also, a collocation method is computationally more efficient than a Galerkin method.

Table 1. Numerical results for the reflectivity using the proposed Chebyshev collocation method for various ω and R .

ω	R	$N=4$	$N=6$	$N=8$	$N=10$	$N=12$	$N=14$	$N=16$	Ref [4]
0.1	0.1	0.88774	0.88774	0.88774					0.88774 (2)
0.5	0.1	0.93580	0.93580	0.93580					0.93580 (2)
0.9	0.1	0.98677	0.98677	0.98677					0.98677 (2)
0.1	1	0.33692	0.33688	0.33687	0.33687				0.33687 (5)
0.5	1	0.54243	0.54230	0.54228	0.54227	0.54226			0.54226 (6)
0.9	1	0.87809	0.87803	0.87802	0.87801				0.87801 (4)
0.1	10	0.02904	0.02978	0.02966	0.02956	0.02951	0.02948	0.02947	0.02944 (14)
0.5	10	0.17085	0.17207	0.17128	0.17084	0.17062	0.1705	0.17044	0.17032 (14)
0.9	10	0.54837	0.54790	0.54718	0.54676	0.54656	0.54645	0.54639	0.54629 (16)

2.4 Orthogonal Collocation with Chebyshev Basis (Linear Anisotropic Case).

After carefully reviewing several papers, the derivation offered by Thynell and Ozisik [5] appears preferable to other works. Following Thynell and Ozisik [5], the general integral form of the transport equation in spherical coordinates can be expressed as

$$rG_n(r) = 2\pi \int_{x=0}^R \left[Q(x)k_{0n}(r, x) + \frac{\omega}{4\pi} \sum_{m=0}^N a_m G_m(x)k_{mn}(r, x) \right] x dx +$$

$$2\pi r \int_{\mu=0}^1 [(-1)^n e^{\tau\mu} + e^{-\tau\mu}] I^- [R, -\mu_o(r, \mu)] P_n(\mu) e^{-\alpha(R, \tau, \mu)} d\mu, \quad x \in [0, R], \quad n = 0, 1, \dots, N, \quad (34)$$

where the kernel function $k_{mn}(r, x)$ is given by

$$k_{mn}(r, x) = \int_{t=|r-x|}^{r+x} P_m\left(\frac{r^2 - x^2 - t^2}{2xt}\right) P_n\left(\frac{r^2 - x^2 + t^2}{2rt}\right) \frac{e^{-t}}{t} dt, \quad m, n = 0, 1, \dots, N, \quad (35)$$

while

$$\alpha(x, r, \mu) = \sqrt{x^2 - r^2(1 - \mu^2)}, \quad (36)$$

and

$$\mu_o(r, \mu) = \sqrt{1 - (r/R)^2(1 - \mu^2)}, \quad (37)$$

Assuming a transparent boundary at $r = R$ allows us to write the boundary condition [7]

$$I^-(R, -\mu) = f(\mu), \quad \mu > 0. \quad (38)$$

Here, the conventional form of the phase function is assumed; namely,

$$p(\mu, \mu') = \sum_{m=0}^N a_m P_m(\mu) P_m(\mu'), \quad a_0 = 1, \quad (39)$$

where the $\{a_m\}_{m=0}^N$ are known coefficients.

For linear anisotropic scattering, $N = 1$, therefore we can express Eq. (36) explicitly as a system of coupled weakly-singular Fredholm integral equations of the second kind. Thus, knowing $P_0(\mu) = 1$, $P_1(\mu) = \mu$ and assuming $\rho_1^s = \rho_1^d = 0$, $T(\mu) = 1$, $A = 0$, and an isotropic external source, $f(\mu) = f$ [5], we find

$$\begin{aligned} rG_0(r) = 2\pi \int_{x=0}^R [Q(x)k_{00}(r, x) + \frac{\omega}{4\pi} \sum_{m=0}^1 a_m G_m(x)k_{m0}(r, x)] x dx + \\ 4\pi r \int_{\mu=0}^1 \cosh(r\mu) e^{-\alpha(R, r, \mu)} f d\mu, \end{aligned} \quad (40)$$

and

$$\begin{aligned} rG_1(r) = 2\pi \int_{x=0}^R [Q(x)k_{01}(r, x) + \frac{\omega}{4\pi} \sum_{m=0}^1 a_m G_m(x)k_{m1}(r, x)] x dx - \\ 4\pi r \int_{\mu=0}^1 \sinh(r\mu) e^{-\alpha(R, r, \mu)} f \mu d\mu, \end{aligned} \quad (41)$$

Next, we map Eqs. (40,41) into a convenient form for the introduction of the Chebyshev basis functions. Let

$$\tau = \lambda(1 + \eta), \quad \tau \in [0, R], \quad \eta \in [-1, 1], \quad (42)$$

where $\lambda = R/2$. Making use of the independent variable transformation offered in Eq. (1.4.4), the system of linear Fredholm equations displayed in Eqs. (1.4.3a,b) become

$$\lambda(1 + \eta)\Phi_0(\eta) = 2\pi\lambda^2 \int_{\xi=-1}^1 [\hat{Q}(\xi)K_{00}(\eta, \xi) + \frac{\omega}{4\pi} \sum_{m=0}^1 a_m \Phi_m(\xi)K_{m0}(\eta, \xi)] (1 + \xi) d\xi +$$

$$4\pi f\lambda(1+\eta) \int_{\mu=0}^1 \cosh[\lambda(1+\eta)\mu] e^{-\alpha(R, \lambda(1+\eta), \mu)} d\mu, \quad (43)$$

and

$$\begin{aligned} \lambda(1+\eta)\Phi_1(\eta) &= 2\pi\lambda^2 \int_{\xi=-1}^1 [\hat{Q}(\xi)K_{01}(\eta, \xi) + \frac{\omega}{4\pi} \sum_{m=0}^1 a_m \Phi_m(\xi)K_{m1}(\eta, \xi)](1+\xi)d\xi - \\ &4\pi f\lambda(1+\eta) \int_{\mu=0}^1 \sinh[\lambda(1+\eta)\mu] e^{-\alpha(R, \lambda(1+\eta), \mu)} \mu d\mu, \end{aligned} \quad (44)$$

where

$$\Phi_m(\eta) = G_m(\lambda(1+\eta)), \quad (45)$$

$$\hat{Q}(\eta) = Q(\lambda(1+\eta)), \quad (46)$$

$$K_{mn}(\eta, \xi) = k_{mn}(\lambda(1+\eta), \lambda(1+\xi)). \quad (47)$$

The coupled Fredholm integral equations are in a proper form for the introduction of the Chebyshev basis. Let

$$\Phi_0(\eta) = \sum_{j=0}^{\infty} b_j T_j(\eta) \approx \Phi_0^{N_0} = \sum_{j=0}^{N_0} b_j^{N_0} T_j(\eta), \quad (48)$$

and

$$\Phi_1(\eta) = \sum_{j=0}^{\infty} c_j T_j(\eta) \approx \Phi_1^{N_1} = \sum_{j=0}^{N_1} c_j^{N_1} T_j(\eta), \quad (49)$$

where $T_j(\eta)$ represents the j^{th} Chebyshev polynomial of the first kind. (Note: it is not necessary that $N_0 = N_1$.) For convenience, we let $N_0 = N_1 = N$. Upon substituting the approximations shown in Eqs. (34,35) into Eqs. (43,44), we form the corresponding residual equations for the system of interest; namely,

$$\begin{aligned} R_0^N(\eta) &= -\lambda(1+\eta)\Phi_0^N(\eta) + \frac{\omega\lambda^2}{2} \left(a_0 \int_{\xi=-1}^1 \Phi_0^N(\xi) K_{00}(\eta, \xi)(1+\xi)d\xi + \right. \\ &\left. a_1 \int_{\xi=-1}^1 \Phi_1^N(\xi) K_{10}(\eta, \xi)(1+\xi)d\xi \right) + \hat{g}_0(\eta), \end{aligned} \quad (50)$$

and

$$\begin{aligned} R_1^N(\eta) &= -\lambda(1+\eta)\Phi_1^N(\eta) + \frac{\omega\lambda^2}{2} \left(a_0 \int_{\xi=-1}^1 \Phi_0^N(\xi) K_{01}(\eta, \xi)(1+\xi)d\xi + \right. \\ &\left. a_1 \int_{\xi=-1}^1 \Phi_1^N(\xi) K_{11}(\eta, \xi)(1+\xi)d\xi \right) + \hat{g}_1(\eta), \end{aligned} \quad (51)$$

where

$$\hat{g}_0(\eta) = g_0(\eta) + 2\pi\lambda^2 \int_{\xi=-1}^1 \hat{Q}(\xi)(1+\xi)K_{00}(\eta, \xi)d\xi, \quad (52)$$

$$\hat{g}_1(\eta) = g_1(\eta) + 2\pi\lambda^2 \int_{\xi=-1}^1 \hat{Q}(\xi)(1+\xi)K_{01}(\eta, \xi)d\xi, \quad (53)$$

$$g_0(\eta) = 4\pi f\lambda(1+\eta) \int_{\mu=0}^1 \cosh[\lambda(1+\eta)\mu]e^{-\alpha(R, \lambda(1+\eta), \mu)}d\mu, \quad (54)$$

$$g_1(\eta) = -4\pi f\lambda(1+\eta) \int_{\mu=0}^1 \sinh[\lambda(1+\eta)\mu]\mu e^{-\alpha(R, \lambda(1+\eta), \mu)}d\mu, \quad (55)$$

where it is understood that $R_j^N(\eta)$, $j = 0, 1$ represents the residual functions.

The collocation method is defined through the following orthogonality statement [11]

$$\langle R_i^N(\eta), \delta(\eta - \eta_k) \rangle_1 = 0, \quad k = 0, 1, \dots, N, \quad (56)$$

where the collocation points η_k can be defined (preliminary) through the open rule

$$\eta_k = \cos\left(\frac{(2k+1)\pi}{2(N+1)}\right), \quad k = 0, 1, \dots, N. \quad (57)$$

2.5 Orthogonal Collocation with Chebyshev Basis (Anisotropic Case [12]).

A benchmark numerical study has been identified for the linear isotropic scattering problem in a sphere. Most studies consider the spherical shell problem over the solid sphere problem. A careful study was found [12] in the literature. The problem described by Thynell [12] involves a uniform source with a zero boundary condition at the outer radius. Thynell [12] used the integral form of the transport equation and developed his solution based on a Galerkin approach. The expansions for the zeroth and first moments of the intensity was based on polynomials. It is interesting to note that these expansions were not directly used in developing plots of these functions or even in obtaining the hemispherical emissivity. In fact, Thynell apparently obtains results by an additional smoothing process involving the original Fredholm integral equations.

For sake of concreteness, we begin by stating the assumptions used in [1] and reduce our previously developed equations. Let $f = 0$, $\hat{Q}(\eta) = 1 - \omega$, and $a_1 = +2.7, -2.7$ (i.e., Thynell's $g' = 0.9, -0.9$, where $a_1 = 3g'$) allows us for form the equivalent problem stated in Ref. [12] for comparative purposes. Equations (43,44) can be shown to reduce to

$$\lambda(1+\eta)\Phi_0(\eta) = 2\pi\lambda^2 \int_{\xi=-1}^1 [(1-\omega)K_{00}(\eta, \xi) + \frac{\omega}{4\pi} \sum_{m=0}^1 a_m \Phi_m(\xi)K_{m0}(\eta, \xi)](1+\xi)d\xi, \quad (58)$$

and

$$\lambda(1+\eta)\Phi_1(\eta) = 2\pi\lambda^2 \int_{\xi=-1}^1 [(1-\omega)K_{01}(\eta, \xi) + \frac{\omega}{4\pi} \sum_{m=0}^1 a_m \Phi_m(\xi) K_{m1}(\eta, \xi)](1+\xi)d\xi. \quad (59)$$

Introducing the approximations for the dependent variables; namely,

$$\Phi_0(\eta) = \sum_{j=0}^{\infty} b_j T_j(\eta) \approx \Phi_0^{N_0}(\eta) = \sum_{j=0}^{N_0} b_j^{N_0} T_j(\eta), \quad (60)$$

and

$$\Phi_1(\eta) = \sum_{j=0}^{\infty} c_j T_j(\eta) \approx \Phi_1^{N_1}(\eta) = \sum_{j=0}^{N_1} c_j^{N_1} T_j(\eta), \quad (61)$$

where $T_j(\eta)$ represents the j^{th} Chebyshev polynomial of the first kind allows us to formulate the necessary residual equations from which the collocation method can be applied. For convenience, we let $N_0 = N_1 = N$. Upon substituting the approximations shown in Eqs. (60,61) into Eqs. (58,59), we form the corresponding residual equations for the system of interest; namely,

$$R_0^N(\eta) = -\lambda(1+\eta)\Phi_0^N(\eta) + \frac{\omega\lambda^2}{2} \left(a_0 \int_{\xi=-1}^1 \Phi_0^N(\xi) K_{00}(\eta, \xi)(1+\xi)d\xi + a_1 \int_{\xi=-1}^1 \Phi_1^N(\xi) K_{10}(\eta, \xi)(1+\xi)d\xi \right) + \hat{g}_0(\eta), \quad (62)$$

and

$$R_1^N(\eta) = -\lambda(1+\eta)\Phi_1^N(\eta) + \frac{\omega\lambda^2}{2} \left(a_0 \int_{\xi=-1}^1 \Phi_0^N(\xi) K_{01}(\eta, \xi)(1+\xi)d\xi + a_1 \int_{\xi=-1}^1 \Phi_1^N(\xi) K_{11}(\eta, \xi)(1+\xi)d\xi \right) + \hat{g}_1(\eta), \quad (63)$$

where

$$\hat{g}_0(\eta) = 2\pi\lambda^2(1-\omega) \int_{\xi=-1}^1 (1+\xi) K_{00}(\eta, \xi)d\xi, \quad (64)$$

$$\hat{g}_1(\eta) = 2\pi\lambda^2(1-\omega) \int_{\xi=-1}^1 (1+\xi) K_{01}(\eta, \xi)d\xi, \quad (65)$$

since $g_0(\eta) = g_1(\eta) = 0$ (i.e., owing to $f = 0$).

The collocation method is defined through the following orthogonality statement [11]

$$\langle R_i^N(\eta), \delta(\eta - \eta_k) \rangle_1 = 0, \quad k = 0, 1, \dots, N, \quad i = 0, 1, \quad (66)$$

where the collocation points η_k can be defined through the open rule

$$\eta_k = \cos\left(\frac{(2k+1)\pi}{2(N+1)}\right), \quad k = 0, 1, \dots, N. \quad (67)$$

Explicitly stated in terms of the expansions, the resulting system for the unknown expansion coefficients becomes

$$\begin{aligned} \sum_{m=0}^N b_m^N \left[-\lambda(1+\eta_k)T_m(\eta_k) + \frac{\omega\lambda^2 a_0}{2} \int_{\xi=-1}^1 (1+\xi)T_m(\xi)K_{00}(\eta_k, \xi)d\xi \right] + \\ \sum_{m=0}^N c_m^N \left[\frac{\omega\lambda^2 a_1}{2} \int_{\xi=-1}^1 (1+\xi)T_m(\xi)K_{10}(\eta_k, \xi)d\xi \right] = -\hat{g}_0(\eta_k), \end{aligned} \quad (68)$$

and

$$\begin{aligned} \sum_{m=0}^N b_m^N \left[\frac{\omega\lambda^2 a_0}{2} \int_{\xi=-1}^1 (1+\xi)T_m(\xi)K_{01}(\eta_k, \xi)d\xi \right] + \\ \sum_{m=0}^N c_m^N \left[-\lambda(1+\eta_k)T_m(\eta_k) + \frac{\omega\lambda^2 a_1}{2} \int_{\xi=-1}^1 (1+\xi)T_m(\xi)K_{11}(\eta_k, \xi)d\xi \right] = -\hat{g}_1(\eta_k), \\ k = 0, 1, \dots, N. \end{aligned} \quad (69)$$

A system of linear algebraic equations containing $2N+2$ unknowns for the expansion coefficients is obtained from the collocation method. The major computational effort of this method lies in arriving at the numerical values for the integrals displayed in Eqs. (68,69). Once the expansion coefficients are determined, reconstruction of $\Phi_0^N(\eta)$ and $\Phi_1^N(\eta)$ is obtained through Eqs. (60,61), respectively.

Tables 2 and 3 present numerical results for the so-called hemispherical emissivity as defined by [12]

$$\epsilon = \frac{\Phi_1(1)}{\pi}, \quad (70)$$

for two optical thicknesses ($R = 1, 5$) where $\lambda = R/2$, two linearly anisotropic scattering phase functions ($a_1 = -2.7, 2.7$) and for three distinct albedos ω . These tables also indicate the number of terms N retained in the finite series representations for $\Phi_0^N(\eta)$ and $\Phi_1^N(\eta)$. Here $a_1 = 3g'$ where g' is used by Thynell [12]. As noted by Thynell [12] and observed here, convergence to an accurate spatial distribution for both $\Phi_0^N(\eta)$ and $\Phi_1^N(\eta)$ is rapid and fairly independent of R, ω, a_1 . It should be noted that the mathematical description for the phase function can drastically change the spatial distribution of both $\Phi_0^N(\eta)$ and $\Phi_1^N(\eta)$.

Tables 4 through 7 present the expansion coefficients, b_j^N and c_j^N required for obtaining $\Phi_0^N(\eta)$ and $\Phi_1^N(\eta)$ when $R = 1, 5$; $\omega = 0.5$, and $a_1 = -2.7$. It should be noted that the basis functions are bounded by unity, i.e., $|T_j(\eta)| < 1$ and thus the significance of the expansion coefficients required in developing $\Phi_0^N(\eta)$ and $\Phi_1^N(\eta)$ can be evaluated. The coupling effect

among the coefficients is evident. Also, qualitative convergence in the numerical value for the expansion coefficients become clear as N is increased.

Figures 1 and 2 present the spatial distributions of $\Phi_0^N(\eta)$ and $\Phi_1^N(\eta)$ when $\omega = 0.5$, $a_1 = -2.7$ and $R = 1, 5$, respectively. It is evident that graphical accuracy is established rapidly. Graphical convergence to accurate solutions for $\Phi_0^N(\eta)$ and $\Phi_1^N(\eta)$ is reached when $N = 8$ for $R = 1$ and $N = 10$ for $R = 5$. It should be noted that the majority of the computational effort needed in the proposed procedure lies in performing the integrations displayed in Eqs. (68,69).

Table 2. Comparison of results for the emissivity, ϵ using the proposed method with that of a Galerkin solution [12] when $R = 1$ for various ω and N .

ω	N	$a_1 = -2.7$	$a_1 = 2.7$
0.1	4	0.656129	0.665831
	8	0.658149	0.667812
	12	0.658311	0.667973
	Exact	0.658359	0.668021
0.5	4	0.444454	0.469481
	8	0.445653	0.470625
	12	0.445756	0.470728
	Exact	0.445788	0.470760
0.9	4	0.11997	0.123487
	8	0.120238	0.123775
	12	0.120264	0.123781
	Exact	0.120273	0.123789

Table 3. Comparison of results for the emissivity, ϵ using the proposed method with that of a Galerkin solution [12] when $R = 5$ for various ω and N .

ω	N	$a_1 = -2.7$	$a_1 = 2.7$
0.1	5	0.907208	0.947699
	10	0.93191	0.970297
	15	0.933751	0.972101
	20	0.934103	0.972451
	Exact	0.934284	0.972631
0.5	5	0.70546	0.890032
	10	0.721914	0.90223
	15	0.723144	0.903432
	20	0.72339	0.903681
	Exact	0.723522	0.903817
0.9	5	0.323634	0.455971
	10	0.327394	0.460083
	15	0.327792	0.460546
	20	0.327877	0.460646
	Exact	0.327928	0.460706

Table 4. Expansion coefficients for $\Phi_0(\eta)$ when $R = 1$, $a_1 = -2.7$, and $\omega = 0.5$.

j	$b_j^N, N = 4$	$b_j^N, N = 8$	$b_j^N, N = 12$
0	4.86016	4.85804	4.85771
1	-1.72849	-1.73392	-1.73467
2	-0.596946	-0.603895	-0.60471
3	-0.123983	-0.133823	-0.134752
4	-0.0403582	-0.056169	-0.0572673
5		-0.0268265	-0.0281706
6		-0.0144178	-0.0161221
7		-0.00770068	-0.00992538
8		-0.00337749	-0.0063966
9			-0.00419902
10			-0.00271823
11			-0.00163689
12			-0.000768877

Table 5. Expansion coefficients for $\Phi_1(\eta)$ when $R = 1$, $a_1 = -2.7$, and $\omega = 0.5$.

j	c_j^N , $N = 4$	c_j^N , $N = 8$	c_j^N , $N = 12$
0	0.633728	0.633851	0.633855
1	0.683529	0.683839	0.68385
2	0.0628458	0.0632614	0.0632769
3	0.0145621	0.0152693	0.015288
4	0.00162813	0.00261631	0.00263845
5		0.000831802	0.000861553
6		0.000294054	0.000331084
7		0.0000954815	0.000151107
8		-0.000000463261	0.0000746734
9			0.0000375295
10			0.0000176865
11			0.00000463922
12			-0.00000441205

Table 6. Expansion coefficients for $\Phi_0(\eta)$ when $R = 5$, $a_1 = -2.7$, and $\omega = 0.5$.

j	b_j^N , $N = 5$	b_j^N , $N = 10$	b_j^N , $N = 20$
0	10.6347	10.6287	10.6274
1	-2.94051	-2.95386	-2.95645
2	-1.73385	-1.75132	-1.75414
3	-0.831056	-0.85626	-0.859423
4	-0.364259	-0.399347	-0.402927
5	-0.131184	-0.190301	-0.19442
6		-0.0989	-0.103734
7		-0.0557601	-0.0615263
8		-0.0327512	-0.0398129
9		-0.0186327	-0.0273765
10		-0.00836338	-0.0196322
11			-0.0144993
12			-0.0109325
13			-0.00835725
14			-0.00643439
15			-0.00495419
16			-0.00377851
17			-0.00281609
18			-0.00199941
19			-0.00128297
20			-0.00062252

Table 7. Expansion coefficients for $\Phi_1(\eta)$ when $R = 5$, $a_1 = -2.7$, and $\omega = 0.5$.

j	$c_j^N, N = 5$	$c_j^N, N = 10$	$c_j^N, N = 20$
0	0.550292	0.551624	0.55166
1	0.876375	0.879222	0.879314
2	0.480069	0.484099	0.484231
3	0.21294	0.217996	0.218168
4	0.0768236	0.0843997	0.0846063
5	0.0197682	0.0313689	0.0316238
6		0.0118365	0.012136
7		0.00476263	0.00514869
8		0.00198648	0.00245649
9		0.000693731	0.00130416
10		-0.0000276501	0.000749993
11			0.000456405
12			0.000289022
13			0.000187398
14			0.000122979
15			0.0000795706
16			0.0000496023
17			0.0000268658
18			0.00000958812
19			-0.0000050528
20			-0.0000176013

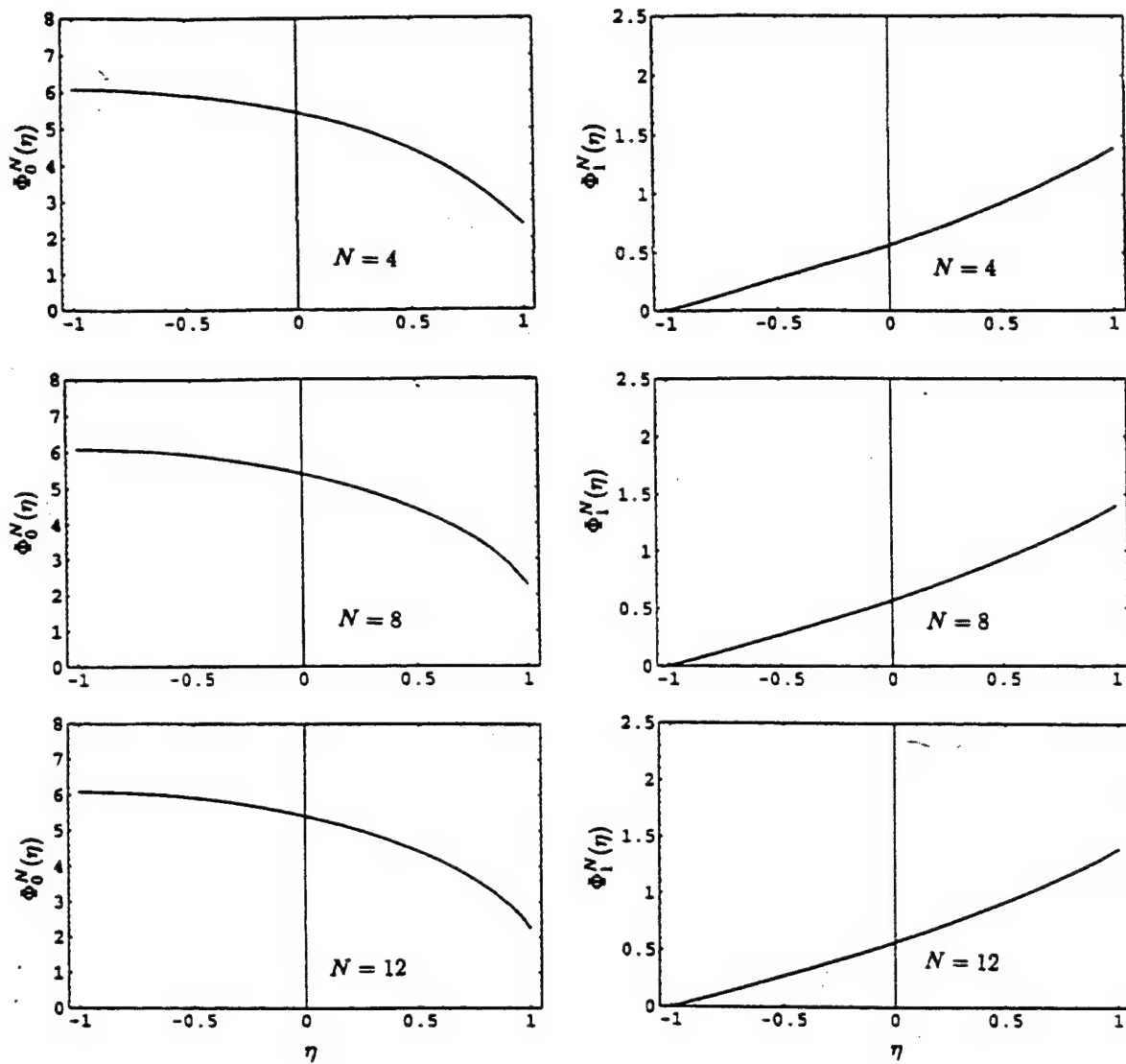


Figure 1. $\Phi_0(\eta)$ and $\Phi_1(\eta)$ distributions for various values of N when $\omega = 0.5$, $a_1 = -2.7$ and $R = 1$.

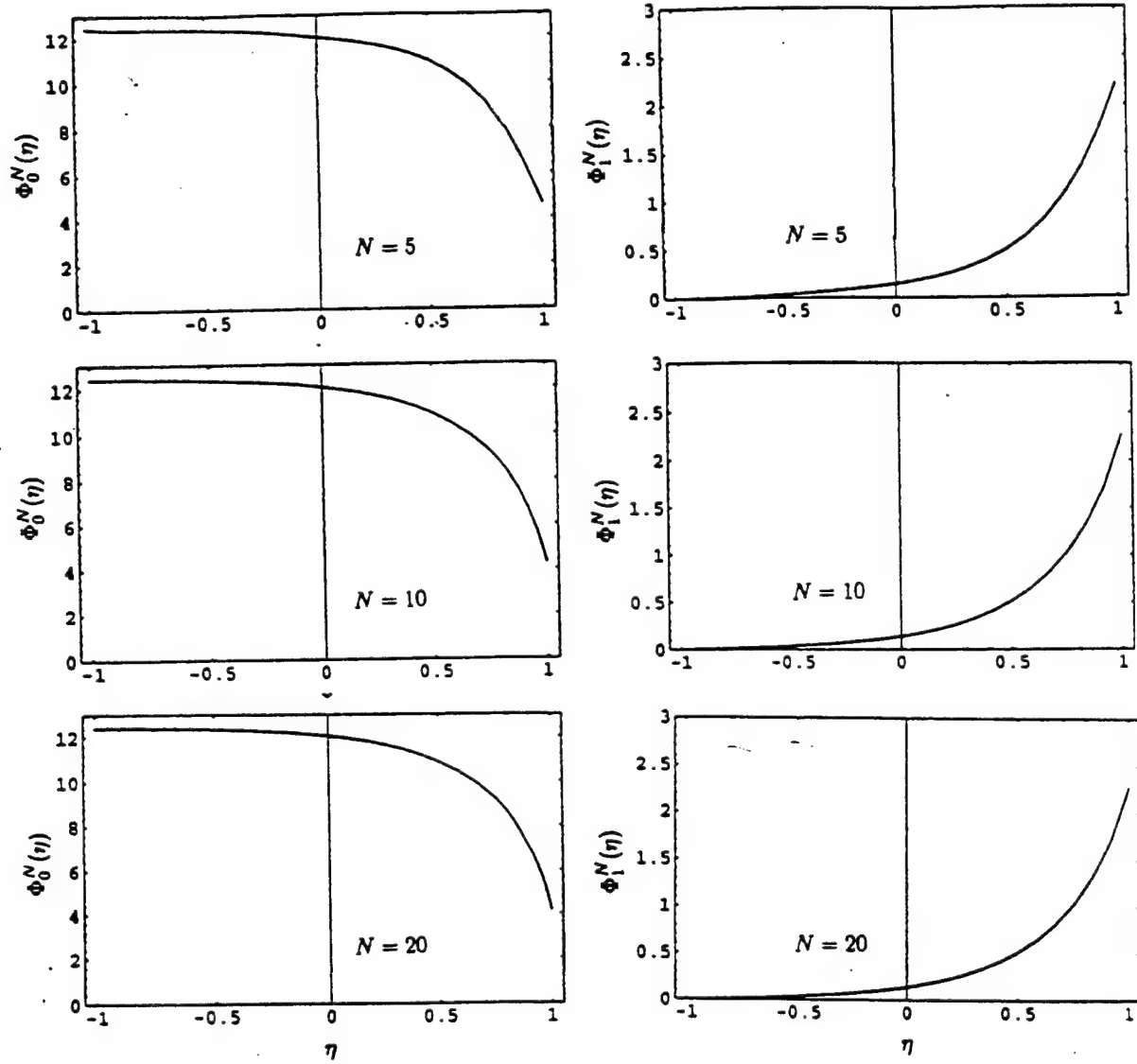


Figure 2. $\Phi_0(\eta)$ and $\Phi_1(\eta)$ distributions for various values of N when $\omega = 0.5$, $a_1 = -2.7$ and $R = 5$.

Section 3 Symbolic-Manipulation of the Kernel Functions

3.1 Identification of the Kernel in Terms of Known Functions.

In this chapter, we document how to express an highly anisotropic scattering phase function in terms of *exponential integral functions and incomplete Gamma functions* by means of symbolic manipulation. This key point now permits the integral form of the transport equation to be used in benchmarking purely numerical solutions. A major objective involves expressing the kernel function in a way that allows for the accurate integration of the angular variable to be performed. This kernel $K_{mn}(\eta, \xi)$ was previously given in terms of a complicated integral involving products of Legendre polynomials having nontrivial arguments. The ability to represent the kernel in this new analytically integrated form is of paramount importance for benchmarking.

3.2 General Anisotropic Scattering Cases.

Previously, we expressed the integral form of the one-speed transport equation as

$$\begin{aligned} rG_n(r) = 2\pi \int_{x=0}^R \left[Q(x)k_{0n}(r, x) + \frac{\omega}{4\pi} \sum_{m=0}^N a_m G_m(x)k_{mn}(r, x) \right] x dx + \\ 2\pi r \int_{\mu=0}^1 [(-1)^n e^{r\mu} + e^{-r\mu}] I^- [R, -\mu_o(r, \mu)] P_n(\mu) e^{-\alpha(R, r, \mu)} d\mu, \\ x \in [0, R], \quad n = 0, 1, \dots, N, \end{aligned} \quad (71)$$

where the kernel function $k_{mn}(r, x)$ is given by

$$k_{mn}(r, x) = \int_{t=|r-x|}^{r+x} P_m\left(\frac{r^2 - x^2 - t^2}{2xt}\right) P_n\left(\frac{r^2 - x^2 + t^2}{2rt}\right) \frac{e^{-t}}{t} dt, \quad m, n = 0, 1, \dots, N, \quad (72)$$

while

$$\alpha(x, r, \mu) = \sqrt{x^2 - r^2(1 - \mu^2)}, \quad (73)$$

and

$$\mu_o(r, \mu) = \sqrt{1 - (r/R)^2(1 - \mu^2)}, \quad (74)$$

Assuming a transparent boundary at $r = R$ allows us to write the boundary condition

$$I^-(R, -\mu) = f(\mu), \quad \mu > 0. \quad (75)$$

Here, the conventional form of the phase function is assumed; namely,

$$p(\mu, \mu') = \sum_{m=0}^N a_m P_m(\mu) P_m(\mu'), \quad a_0 = 1, \quad (76)$$

where the $\{a_m\}_{m=0}^N$ are known coefficients and $P_m(\mu)$ represents the m^{th} Legendre polynomial of the first kind.

Next, we map Eqs. (71-74) into a convenient form for the introduction of the Chebyshev basis functions. Let

$$r = \lambda(1 + \eta), \quad r \in [0, R], \quad \eta \in [-1, 1], \quad (77)$$

where $\lambda = R/2$. Making use of the independent variable transformation defined in Eq. (77), the system of linear Fredholm equations displayed in Eq. (71-74) becomes

$$\begin{aligned} \lambda(1 + \eta)\Phi_n(\eta) = & 2\pi\lambda^2 \int_{\xi=-1}^1 \left[\hat{Q}(\xi)K_{0n}(\eta, \xi) + \frac{\omega}{4\pi} \sum_{m=0}^N a_m \Phi_m(\xi)K_{mn}(\eta, \xi) \right] (1 + \xi)d\xi + \\ & 2\pi\lambda(1 + \eta) \int_{\mu=0}^1 f(\mu)P_n(\mu)[(-1)^n e^{\lambda(1+\eta)\mu} + e^{-\lambda(1+\eta)\mu}] e^{-\alpha(R, \lambda(1+\eta), \mu)} d\mu, \\ & n = 0, 1, \dots, N, \end{aligned} \quad (78)$$

where

$$\Phi_m(\eta) = G_m(\lambda(1 + \eta)), \quad (79)$$

$$\hat{Q}(\eta) = Q(\lambda(1 + \eta)), \quad (80)$$

$$K_{mn}(\eta, \xi) = k_{mn}(\lambda(1 + \eta), \lambda(1 + \xi)), \quad (\eta, \xi) \in [-1, 1], \quad (81)$$

with the kernel function as

$$\begin{aligned} K_{mn}(\eta, \xi) = & \int_{t=\lambda|\eta-\xi|}^{\lambda(2+\eta+\xi)} P_m\left(\frac{\lambda^2(1+\eta)^2 - \lambda^2(1+\xi)^2 - t^2}{2\lambda(1+\xi)t}\right) P_n\left(\frac{\lambda^2(1+\eta)^2 - \lambda^2(1+\xi)^2 + t^2}{2\lambda(1+\eta)t}\right) \frac{e^{-t}}{t} dt, \\ & m, n = 0, 1, \dots, N, \quad (\eta, \xi) \in [-1, 1]. \end{aligned} \quad (82)$$

Equation (78) represents a system of $N+1$ linear Fredholm integral equations of the second kind. These equations are in a proper form for the introduction of the Chebyshev basis.

3.3 Identification of $K_{mn}(\eta, \xi)$ in Terms of Known Functions.

The kernel function shown in Eq. (82) in terms of exponential integral functions and incomplete Gamma functions with the aid of symbolic manipulation. That is, we have identified and expressed the product of the Legendre polynomials shown in Eq. (82) as

$$\begin{aligned} & \sum_{i=-(m+n)}^{m+n} F_i^{mn}(\eta, \xi) t^i = \\ & P_m\left(\frac{\lambda^2(1+\eta)^2 - \lambda^2(1+\xi)^2 - t^2}{2\lambda(1+\xi)t}\right) P_n\left(\frac{\lambda^2(1+\eta)^2 - \lambda^2(1+\xi)^2 + t^2}{2\lambda(1+\eta)t}\right), \\ & m, n = 0, 1, \dots, N. \end{aligned} \quad (83)$$

This rather complicated RHS is now expressed in terms of positive and negative integer exponents in t having a variable coefficient set denoted by $F_i^{mn}(\eta, \xi)$. These variable coefficients can be determined through symbolic computation. Upon substituting Eq. (83) into Eq. (82), we find

$$K_{mn}(\eta, \xi) = \sum_{i=-(m+n)}^{m+n} F_i^{mn}(\eta, \xi) \int_{t=\lambda|\eta-\xi|}^{\lambda(2+\eta+\xi)} t^{i-1} e^{-t} dt. \quad (84)$$

This *new* form is quite amenable to further interpretation. Before proceeding further, we state two integral relations that will be used. It can be shown that

$$\int_{t=z}^y \frac{e^{-t}}{t^p} dt = \frac{E_p(z)}{z^{p-1}} - \frac{E_p(y)}{y^{p-1}}, \quad p = 1, 2, \dots, \quad (85)$$

and

$$\int_{t=z}^y t^{p-1} e^{-t} dt = \Gamma(p, z) - \Gamma(p, y), \quad p = 1, 2, \dots \quad (86)$$

Here, $E_p(u)$ represents the exponential integral function of p^{th} order and $\Gamma(p, u)$ represents the p^{th} incomplete Gamma function. For convenience, we define

$$\hat{z}(\eta, \xi) = \lambda|\eta - \xi|, \quad (87)$$

$$\hat{y}(\eta, \xi) = \lambda(2 + \eta + \xi), \quad (88)$$

thus, the kernel function shown in Eq. (84) may be written as

$$K_{mn}(\eta, \xi) = \sum_{i=-(m+n)}^0 F_i^{mn}(\eta, \xi) \int_{t=\hat{z}(\eta, \xi)}^{\hat{y}(\eta, \xi)} t^{i-1} e^{-t} dt + \sum_{i=1}^{m+n} F_i^{mn}(\eta, \xi) \int_{t=\hat{z}(\eta, \xi)}^{\hat{y}(\eta, \xi)} t^{i-1} e^{-t} dt, \quad m, n = 0, 1, \dots, N. \quad (89)$$

In the first summation, replace $-i$ by i to get

$$K_{mn}(\eta, \xi) = \sum_{i=0}^{m+n} F_{-i}^{mn}(\eta, \xi) \int_{t=\hat{z}(\eta, \xi)}^{\hat{y}(\eta, \xi)} \frac{e^{-t}}{t^{i+1}} dt + \sum_{i=1}^{m+n} F_i^{mn}(\eta, \xi) \int_{t=\hat{z}(\eta, \xi)}^{\hat{y}(\eta, \xi)} t^{i-1} e^{-t} dt, \quad m, n = 0, 1, \dots, N, \quad (\eta, \xi) \in [-1, 1]. \quad (90)$$

Using the integrals shown in Eqs. (85,86), we observe that the kernel $K_{mn}(\eta, \xi)$ can be expressed as

$$\dot{K}_{mn}(\eta, \xi) = \sum_{i=0}^{m+n} F_i^{mn}(\eta, \xi) \left(\frac{E_{i+1}(\hat{z}(\eta, \xi))}{\hat{z}^i(\eta, \xi)} - \frac{E_{i+1}(\hat{y}(\eta, \xi))}{\hat{y}^i(\eta, \xi)} \right) +$$

$$\sum_{i=1}^{m+n} F_i^{mn}(\eta, \xi) \left(\Gamma[i, \hat{z}(\eta, \xi)] - \Gamma[i, \hat{y}(\eta, \xi)] \right), \quad m, n = 0, 1, \dots, N, \quad (\eta, \xi) \in [-1, 1]. \quad (91)$$

This representation is correct but does appear to cause some numerical difficulties when m, n are greater than or equal to 2. It was found that the evaluations using *Mathematica*TM version 2.2 took an excessive amount of CPU time on a SGI and that some numerical inaccuracies appeared in the higher moments. Scrutinizing this occurrence permitted us to make several observations including: (1) the geometric singularity caused problems near $\eta = -1$ (i.e., $r = 0$); and, (2) the strength of the singularity in the kernel functions at $\eta = \xi$ grows with the degree of anisotropy. The first identified problem can be corrected by modifying (tailoring) the trial functions. The second problem has been partially addressed. However, the second problem has been substantially reduced and we are presently addressing the region about $\eta = \xi$ in the kernel function $K_{mn}(\eta, \xi)$ in a focused manner.

The highly successful results involving anisotropic scatter in the slab geometry and our previously reported work involving linear anisotropic scattering in spheres do not immediately translate to the corresponding spherical case when $n \geq 2$. Thus, a major effort of the research program involved performing extremely difficult integrations in an accurate and efficient manner. Once this is resolved, the computational procedure is quite clear.

3.4 Modified Kernel Approach.

In order to reduce the observed numerical difficulties associated with our previous derivation, we offer the following re-packaging concept. We express Eq. (82) as

$$K_{mn}(\eta, \xi) = K_{mn}(\eta, \xi) \pm \int_{t=\lambda|\eta-\xi|}^{\lambda(2+\eta+\xi)} P_m\left(\frac{-t}{2\lambda(1+\eta)}\right) P_n\left(\frac{t}{2\lambda(1+\eta)}\right) \frac{e^{-t}}{t} dt, \quad m, n = 0, 1, \dots, N, \quad (\eta, \xi) \in [-1, 1], \quad (92)$$

and regroup with the hopes of reducing the problem in the vicinity about $\eta = \xi$. Regrouping terms in Eq. (92) permits us to express $K_{mn}(\eta, \xi)$ as

$$K_{mn}(\eta, \xi) = \bar{K}_{mn}(\eta, \xi) + \dot{K}_{mn}(\eta, \xi), \quad (93)$$

where

$$\bar{K}_{mn}(\eta, \xi) = \int_{t=\hat{z}(\eta, \xi)}^{\hat{y}(\eta, \xi)} \left[P_m\left(\frac{\lambda^2(1+\eta)^2 - \lambda^2(1+\xi)^2 - t^2}{2\lambda(1+\xi)t}\right) P_n\left(\frac{\lambda^2(1+\eta)^2 - \lambda^2(1+\xi)^2 + t^2}{2\lambda(1+\eta)t}\right) - \right.$$

$$P_m\left(\frac{-t}{2\lambda(1+\eta)}\right)P_n\left(\frac{t}{2\lambda(1+\eta)}\right)\left]\frac{e^{-t}}{t}dt, \quad m, n = 0, 1, \dots, N, \quad (\eta, \xi) \in [-1, 1]. \quad (94)$$

and

$$\hat{K}_{mn}(\eta, \xi) = \int_{t=\hat{z}(\eta, \xi)}^{\hat{y}(\eta, \xi)} P_m\left(\frac{-t}{2\lambda(1+\eta)}\right)P_n\left(\frac{t}{2\lambda(1+\eta)}\right)\frac{e^{-t}}{t}dt, \quad m, n = 0, 1, \dots, N, \quad (\eta, \xi) \in [-1, 1]. \quad (95)$$

These expressions can be simplified in a similar manner as previously discussed; namely, we find

$$\begin{aligned} \bar{K}_{mn}(\eta, \xi) = & \sum_{i=0}^{m+n} f_i^{(m,n)}(\eta, \xi) \left[\frac{E_{i+1}(\hat{z}(\eta, \xi))}{\hat{z}^i(\eta, \xi)} - \frac{E_{i+1}(\hat{y}(\eta, \xi))}{\hat{y}^i(\eta, \xi)} \right] + \\ & \sum_{i=1}^{m+n} f_i^{(m,n)}(\eta, \xi) \left[\Gamma(i, \hat{z}(\eta, \xi)) - \Gamma(i, \hat{y}(\eta, \xi)) \right], \end{aligned} \quad (96)$$

and

$$\begin{aligned} \hat{K}_{mn}(\eta, \xi) = & g_0^{(m,n)}(\eta) [E_1(\hat{z}(\eta, \xi)) - E_1(\hat{y}(\eta, \xi))] + \\ & \sum_{i=1}^{m+n} g_i^{(m,n)}(\eta) [\Gamma(i, \hat{z}(\eta, \xi)) - \Gamma(i, \hat{y}(\eta, \xi))], \end{aligned} \quad (97)$$

where $f_i^{(m,n)}(\eta, \eta) = 0$, for all m, n . Again, these $f_i^{(m,n)}(\eta, \xi)$ have similar features to those given by our original $F_i^{(m,n)}(\eta, \xi)$ with the exception of the collapsing behaviour near $\eta = \xi$.

This new kernel representation behaves much better, however there still exists some difficulties. Asymptotic expansions were attempted to alleviate some of the numerical difficulties. However, they did not render enough accuracy. In the last month of the program, a literature survey revealed that some recent work in the area of Finite Integral Part Integration (in the sense of Hadamard) may assist in resolving the final dilemma. Unfortunately, the contractual period has closed and the financial resources are not available to continue the project.

3.5 Identified Anisotropic Scattering Test Phase Function.

The traditional scattering phase function is expressed in terms of Legendre polynomials of the first kind; namely.

$$p_n(\mu, \mu') = \sum_{j=0}^n a_j P_j(\mu) P_j(\mu'), \quad (98)$$

where $\{a_j\}_{j=0}^n$ represent known coefficients. For example, if $a_0 = 1$, $a_1 = -0.56524$, $a_2 = 0.29783$, $a_3 = 0.08571$, $a_4 = 0.01003$, $a_5 = 0.00063$, then the phase function can be graphically displayed as shown in Figure 3. This particular phase function has been used often. It should be noted that by changing the last coefficient to $a_5 = 0.800063$ a drastic change occurs in the resulting phase function as shown in Figure 4. This test phase function appears to offer several features worthy in a simulation.

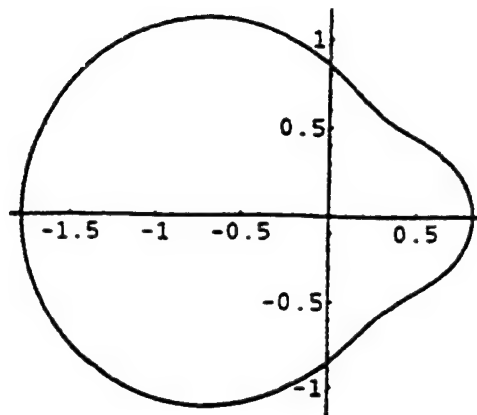


Figure 3. Simple backscattering phase function.

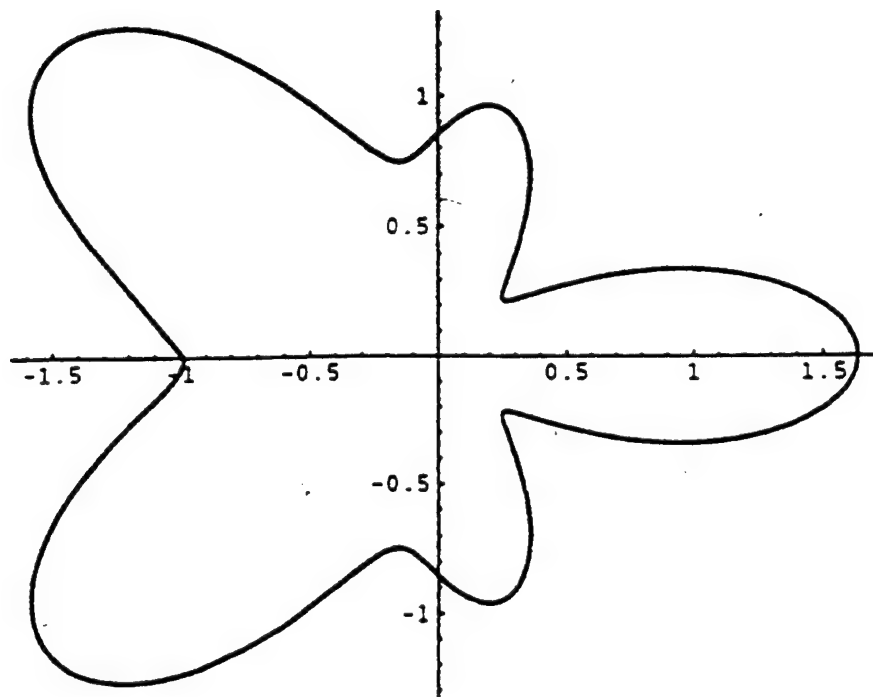


Figure 4. Highly lobular phase function.

Section 4

Conclusions and Recommendations

The last significant technical issue involved handling, in a general manner, the numerical singularity that appears at the origin as the degree of anisotropy is increased. In a general sense, this is a rather substantial problem that apparently has not been addressed in the literature. For example, though Thynell and Ozisik [5] developed the general one-dimensional integral form of the transport equation for the solid sphere, they do not identify any potential numerical problems that could occur. In a follow-up paper by Thynell [13], the author limits his discussion to the trivial problem of linear-anisotropic scattering. Likewise, Abulwafa [6] investigates the case of highly anisotropic scattering by recasting it into a linear-anisotropic form (an approximation). In this way, the author could obtain numerical results.

In the planar geometry (a nonsingular geometry), our symbolically enhanced methodology has been demonstrated to work extremely well (see [4]). This was again indicated during the first year of this two-year program. In the case of isotropic and linear-anisotropic scattering, again the approach has been demonstrated to work extremely well. This was demonstrated during the first half of the second year of the two-year program. The last significant task involved the final generalization to highly anisotropic scattering. A general and novel expression has been derived indicating that a severe numerical singularity is present at the origin for a solid sphere. A significant effort has been underway to resolve this final technical issue. As of this report, this final obstacle has not been overcome. This last hurdle appears resolvable and may have been considered by other researchers in different areas.

The development of analytic methods in fracture mechanics and the boundary integral method may lead to the proper handling of such integrals. These integrals are strongly singular in the sense of Hadamard [14-17] and involve the so-called finite integral part. Strongly singular kernels of this type have appeared, in recent years, in the study of hypersingular integral equations (boundary element method) and applications involving fracture mechanics. The final clue on the proper resolution of singularities associated with the spherical problem may be assisted by investigating these other areas.

The major recommendation offered by this investigator involves providing resources to understand how the investigation of strongly singular kernels associated with fracture mechanics and hypersingular integral equations can be used to resolve the final research issue associated with this study. Once this is resolved, the numerical procedure for determining the solution of the resulting system of Fredholm integral equations is well established and no major hurdle is foreseen.

Section 5
References

1. Frankel, J.I., "Computational attributes of the integral form of the equation of transfer", **JQSRT**, vol. 58, 1991, pp. 329-342 (UNCLASSIFIED).
2. Frankel, J.I., "Several symbolic augmented Chebyshev expansion for solving the equation of radiative transfer", **J. Computational Physics**, vol. 117, 1995, pp. 350-363 (UNCLASSIFIED).
3. LaClair, T. and J.I. Frankel, "Chebyshev series solution for radiative transport in a medium with a linearly anisotropic scattering phase function", **Int. J. Numerical Methods for Heat Transfer and Fluid Flow**, vol. 5, 1995, pp. 685-704 (UNCLASSIFIED).
4. Frankel, J.I., "Final Report-DAHC35-95-P-3171-An innovative computational method for predicting neutron transport: proof-of-principle", March 1996 (UNCLASSIFIED).
5. Thynell, S.T., and M.N. Ozisik, "The integral form of the equation of radiative transfer for an inhomogeneous anisotropically scattering, solid sphere", **IMA Journal of Applied Mathematics**, vol. 34, 1985, pp. 323-328 (UNCLASSIFIED).
6. Abulwafa, E.M., "Radiative-transfer in a linearly-anisotropic spherical medium", **JQSRT**, vol. 49, 1993, pp. 165-175 (UNCLASSIFIED).
7. Thynell, S.T., and M.N. Ozisik, "Radiation transfer in an isotropically scattering solid sphere with space dependent albedo, $\omega(r)$ ", **J. Heat Transfer**, vol. 107, 1985, pp. 732-734 (UNCLASSIFIED).
8. Siewert, C.E., and P. Grandjean, "Three basic neutron-transport problems in spherical geometry", **Nuclear Science and Engineering**, vol. 70, 1979, pp. 96-98 (UNCLASSIFIED).
9. Siewert, C.E., and J.R. Thomas, "Radiative transfer calculations in spheres and cylinders", **JQSRT**, vol. 34, 1985, pp. 59-64 (UNCLASSIFIED).
10. Pomraning, G.C., and C.E. Siewert, "On the integral form of the equation of transfer for a homogeneous sphere", **JQSRT**, vol. 28, 1982, pp. 503-506 (UNCLASSIFIED).
11. Finlayson, B.A., *The Method of Weighted Residuals and Variational Principles*, Academic Press, New York, 1972 (UNCLASSIFIED).
12. Thynell, S.T., "Radiative transfer in absorbing, emitting and linearly anisotropically scattering spherical media", **JQSRT**, vol. 41, 1989, pp. 383-395.
13. Tsai, J.R., M.N. Ozisik, and F. Santarelli, "Radiation in spherical symmetry with anisotropic scattering and variable properties", **JQSRT**, vol. 42, 1989, pp. 187-199 (UNCLASSIFIED).
14. Martin, P.A., "Exact solution of a simple hypersingular integral equation", **J. Integral Equations**, vol. 4, 1992, pp. 197-203 (UNCLASSIFIED).
15. Bertram, B., "On the use of product integration for the solution of finite part singular integral equations", (in *Integral Methods in Science and Engineering-90*), Hemisphere Publishing Corporation, New York, 1991 (UNCLASSIFIED).

16. Kaya, A.C., and F. Erdogan, "On the solution of integral equations with strongly singular kernels", **Quarterly of Appl. Math.**, vol. 95, 1987, pp. 105-122 (UNCLASSIFIED).
17. Kutt, H.R., "The numerical evaluation of principal value integrals by finite part integration", **Numer. Math.**, vol. 24, 1977, pp. 205-210 (UNCLASSIFIED).

Appendix
DAHC35-95-P-3171 [4]

-FINAL REPORT-

DAHC35-95-P-3171

**An Innovative Computational Method
for Predicting Neutron Transport: Proof-of-Principle**

by

J.I. Frankel

Associate Professor

**Mechanical and Aerospace Engineering
and Engineering Sciences Department**

University of Tennessee, Knoxville

Knoxville, Tennessee 37996-2210

e-mail: frankel@titan.engr.utk.edu

Summary

This final report delivers encouraging results indicating the merit of the proposed computational methodology. The preliminary stage involving the past year verifies the concept proposed in the original proposal to DNA. Follow-on funding is now sought to resolve transport questions involving spherical geometries. Each proposed task of the SOW is addressed in a self-contained manner and is presented as a chapter in this final report.

Table of Content

Section	Page
0.0 Report Organization	2
1.0 Task I: Verification of the Computational Methodology	2
1.1 Introduction	2
1.2 Formulation	3
1.3 Solution	4
1.4 Results and Conclusions	6
1.5 References	8
1.6 List of Tables	10
1.7 List of Figures	14
2.0 Task II: Spherical Coordinate Formulation	18
2.1 Introduction	18
2.2 Formulation and Remarks	18
2.3 References	21

0.0 Report Organization

This final report is organized in two major sections. The first section involves addressing Task I while the second portion of the report directly addresses Task II as stated in the Statement of Work. For sake of reference, the tasks as stated in the SOW are:

I) Development of the appropriate mathematical formulation and demonstration of the proposed methodology. Several benchmark cases exist and will be considered as they pertain to slab geometries. The solution methodology will take advantage of symbolic manipulation and a spectral based expansion method for determining the unknown functions of interest.

II) Formulation of the integral form of the Boltzmann transport equation in spherical coordinates in the presence of a highly anisotropic phase function.

Each task is addressed separately and is meant to be self contained.

1.0 Task I: Verification of the Computational Methodology

This portion of the final report addresses Task I as reported in the SOW and described in the Report Organization.

1.1 Introduction

In a series of recent articles [1-3], a symbolically enhanced methodology has been developed for solving the integral form of the Boltzmann transport equation in the presence of anisotropy. The integral form of the transport equation has been utilized in these past one-dimensional studies since a reduction in dimensionality takes place. The resulting system of weakly-singular Fredholm integral equations of the second kind arises coupling the various moments of the intensity (radiative transport) or neutron flux (neutron transport).

In [1], an important computational attribute was identified pertaining to the integral form of the transport equation. It was observed that symbolic manipulation can be used to automate the identification of the kernel function needed to arrive at the integral form of the transport equation. Theoretical considerations involving convergence and error analyses were established in [2,3] based on a weighted residual methodology where Chebyshev polynomials were used as the basis functions in the expansions. The convergence rate was established for the isotropic scattering case when implementing orthogonal collocation. In [3], LaClair and Frankel investigated linear anisotropic scattering and developed rigorous error estimates based on functional analysis that extended the error estimates developed in [2].

This report presents the actual implementation of symbolic manipulation for automatically setting up the kernel functions needed in the integral form of the transport equation given an arbitrary scattering phase function. Extension to two-dimensional cases now appears feasible. Chebyshev polynomials of the first kind are chosen as the basis set for approximating the unknown Legendre moments. The unknown expansion coefficients

are obtained in a weighted residual sense using orthogonal collocation. Comparisons with existing solutions qualitatively indicate the accuracy of the approach. This form of error evaluation is chosen since a functional analysis approach becomes unwieldy and thus impractical for cases having a high degree of anisotropy.

1.2 Formulation

The general one-dimensional, gray (one-speed), slab formulation follows from previous presentations [1,4] and thus is not derived here. The independent variables are mapped into a coordinate system conducive to the spatial format of the spectral basis functions to be shortly introduced. Using $\tau = \lambda(1+x)$, the derivation developed and described in [1,4] can be expressed in the equivalent form

$$\bar{G}_n(x) = \bar{F}_n(x) + \frac{\lambda\omega}{2} \sum_{m=0}^M a_m \int_{x_o=-1}^1 \bar{K}_{m,n}(\lambda|x-x_o|) \bar{G}_m(x_o) dx_o, \quad n = 0, 1, \dots, M, \quad x \in [-1, 1], \quad (1.1a)$$

where

$$\bar{K}_{m,n}(\lambda|x-x_o|) = \bar{R}_{m,n}(\lambda(x-x_o)) \bar{Q}_{m,n}(\lambda|x-x_o|), \quad (1.1b)$$

where the partial kernel functions are given as

$$\bar{Q}_{m,n}(\lambda|x-x_o|) = \int_{\mu=0}^1 \frac{P_m(\mu)P_n(\mu)}{\mu} e^{\frac{-\lambda|x-x_o|}{\mu}} d\mu, \quad (1.1c)$$

$$\bar{R}_{m,n}(\lambda(x-x_o)) = \begin{cases} 1, & x-x_o > 0; \\ (-1)^{m+n}, & x_o-x > 0, \end{cases} \quad (1.1d)$$

while the mapped forcing function becomes

$$\begin{aligned} \bar{F}_n(x) = 2\pi \int_{\mu=0}^1 P_n(\mu) [I^+(-1, \mu) e^{\frac{-\lambda(1+x)}{\mu}} + (-1)^n I^-(1, -\mu) e^{\frac{-\lambda(1-x)}{\mu}}] d\mu + \\ 2\pi\lambda \int_{x_o=-1}^1 \bar{s}(x_o) \bar{K}_{0,n}(\lambda|x-x_o|) dx_o, \quad x \in [-1, 1], \end{aligned} \quad (1.1e)$$

where $\lambda = \tau_d/2$. In [1], the n^{th} Legendre moment of the intensity (or angular flux) is defined as $G_n(\tau)$ for $\tau \in [0, \tau_d]$ where τ_d is the optical depth. The n^{th} Legendre polynomial of the first kind is denoted as $P_n(\mu)$. Thus, $\bar{G}_n(x) = G_n(\lambda(1+x))$ represents the mapped form of the dependent variable. Here, the coefficients $\{a_m\}_{m=0}^M$ are the prescribed phase function coefficients.

Frankel [1] indicates that symbolic manipulation can be exploited for automating the evaluation of the integral function displayed in Eq. (1.1c) for $\bar{Q}_{m,n}(\lambda|x-x_o|)$ since it is readily recognizable in terms of a finite set of exponential integral functions. In particular, the partial kernel function $\bar{Q}_{m,n}(\lambda|x-x_o|)$ can be expressed as

$$\bar{Q}_{m,n}(\lambda|x-x_o|) = \sum_{j=0}^{\bar{N}_{m,n}-1} c_j^{(m,n)} E_{j+1}(\lambda|x-x_o|), \quad (m,n) = 0, 1, \dots, M, \quad (1.2)$$

where $E_j(z)$ denotes the j^{th} exponential integral function [5]. Given the integer values of m, n from 0 to M , the coefficients $c_j^{(m,n)}$ and number of terms in the sum $\bar{N}_{m,n}$ can be established with the aid of symbolic manipulation without any difficulty. In fact, $\bar{N}_{m,n}$ is known a priori from properties of polynomial multiplication [1]. Figure 1 displays such a cell of code as prepared using the symbolic software package *Mathematica*TM [6] and implemented on a NeXTstation having 16 MBytes of memory. Similar functionality exists on most conventional symbolic manipulators such as Maple and MacSyma. Finally, it should be evident from viewing Eq. (1.1c) that $c_j^{(m,n)} = c_j^{(n,m)}$ and $\bar{N}_{m,n} = \bar{N}_{n,m}$.

The product of the Legendre polynomials $P_m(\mu)$ and $P_n(\mu)$ is formed and denoted as "fmn". Using the intrinsic function, `CoefficientList`, a list is built that contains the coefficients of the resulting multiplication of the two polynomials. The generated list contains the coefficients in ascending order starting with the coefficient for μ^0 and ending with the coefficient for μ^{m+n} . The total length of the list is $m+n+1$. Use of the intrinsic function `Length` counts the number of elements in the generated list. Clearly, this should be equal to $m+n+1$. This result is stored in the array named "arraymaxc" having elements named "maxcoeff[m,n]". The coefficients $c_j^{(m,n)}$ are then constructed and stored for later use. The output portion of the cell indicates the resulting operations to produce $c_j^{(m,n)}$ for the Rayleigh scattering phase function, i.e., $M = 2$, $a_0 = 1$, $a_1 = 0$, and $a_2 = 0.5$. In general, approximately half of the coefficients $c_j^{(m,n)}$ for $j = 0, 1, \dots, \bar{N}_{(m,n)} - 1$ are zero in value for fixed (m, n) .

1.3 Solution

A weighted residual methodology, utilizing orthogonal collocation, has been recently demonstrated to yield accurate results [2,3]. In this section, an orthogonal collocation method is presented for finding an approximate solution to $\bar{G}_n(x)$ as indicated in Eq. (1.1a). Let the unknown function $\bar{G}_n(x)$ be formally represented by the series expansion

$$\bar{G}_n(x) = \sum_{i=0}^{\infty} b_{n,i} T_i(x), \quad x \in [-1, 1], \quad n = 0, 1, \dots, M, \quad (1.3a)$$

where the basis functions $\{T_i(\eta)\}_{i=0}^{\infty}$ are chosen as the Chebyshev polynomials of the first kind [2,3,7] and are expressible as

$$T_i(\eta) = \cos[i(\cos^{-1}\eta)], \quad i = 0, 1, \dots \quad (1.3b)$$

Chebyshev polynomials [7] have numerous exploitable features and have successfully been used in studies involving fluid mechanics [8], solid mechanics [9], and radiative transport [10,11]. The unknown expansion coefficients for each moment, n requiring resolution are denoted as $\{b_{n,i}\}_{i=0}^{\infty}$. In practice, this series representation is truncated after a finite number of terms, say at order N_n , which depends on the particular moment, n . For sake of

simplicity, let $N_n = N$, that is, each moment is approximated by a polynomial of the same order. Thus, the N^{th} -order approximation of $\bar{G}_n(x)$ is denoted as $\bar{G}_n^N(x)$ and expressed by

$$\bar{G}_n(x) \approx \bar{G}_n^N(x) = \sum_{i=0}^N b_{n,i}^N T_i(x), \quad n = 0, 1, \dots, M, \quad (1.4)$$

where $b_{n,i}^N$ represents an approximation to $b_{n,i}$, respectively for each fixed n, i in the finite set.

The series representation shown in Eq. (1.4) for $\bar{G}_n^N(x)$, $n = 0, 1, \dots, M$ is substituted into Eq. (1.1a) to produce

$$R_n^N(x) + \sum_{i=0}^N b_{n,i}^N T_i(x) = \bar{F}_n(x) + \frac{\lambda\omega}{2} \sum_{m=0}^M a_m \sum_{i=0}^N b_{m,i}^N \sum_{j=0}^{\bar{N}_{m,n}-1} c_j^{(m,n)} I_{j+1,i}^{(m,n)}(x),$$

$$n = 0, 1, \dots, M; \quad x \in [-1, 1], \quad (1.5)$$

where $R_n^N(x)$ represents the residual function required to maintain the equality displayed in Eq. (1.5a). The function $I_{j+1,i}^{(m,n)}(x)$ represents the result of the analytic integration of the product of the i^{th} Chebyshev polynomial of the first kind and the kernel function $\bar{K}_{m,n}(\lambda|x-x_o|)$ defined in Eq. (1.1b). That is, upon redefining $\bar{Q}_{m,n}(\lambda|x-x_o|)$ shown in Eq. (1.1c) as Eq. (1.2) and then forming the definition of the kernel, $\bar{K}_{m,n}(\lambda|x-x_o|)$, the function $I_{j+1,i}^{(m,n)}(x)$ is identified as

$$I_{j+1,i}^{(m,n)}(x) = \int_{x_o=-1}^1 \bar{R}_{m,n}(\lambda|x-x_o|) E_{j+1}(\lambda|x-x_o|) T_i(x_o) dx_o,$$

$$j = 0, 1, \dots, \bar{N}_{m,n} - 1; \quad (m, n) = 0, 1, \dots, M; \quad i = 0, 1, \dots, N; \quad x \in [-1, 1]. \quad (1.6a)$$

Integrating Eq. (1.6a) analytically yields

$$I_{j+1,i}^{(m,n)}(x) = \sum_{k=0}^i \frac{T_i^{(k)}(x)}{\lambda^{k+1}} (-1)^k E_{j+k+2}(0) [1 + (-1)^{m+n+k}] +$$

$$\sum_{k=0}^i \frac{1}{\lambda^{k+1}} \left((-1)^{k+1} T_i^{(k)}(-1) E_{j+k+2}(\lambda(1+x)) - (-1)^{m+n} T_i^{(k)}(1) E_{j+k+2}(\lambda(1-x)) \right),$$

$$j = 0, 1, \dots, \bar{N}_{m,n} - 1; \quad (m, n) = 0, 1, \dots, M; \quad i = 0, 1, \dots, N; \quad x \in [-1, 1]. \quad (1.6b)$$

Here, the k^{th} derivative of the p^{th} Chebyshev polynomial of the first kind is denoted as $T_p^{(k)}(x)$.

Unless the exact solution to $\bar{G}_n(x)$, $n = 0, 1, \dots$, is a linear combination of the basis functions $\{T_i(x)\}_{i=0}^{\infty}$, no set of coefficients $b_{n,i}^N$ can make $R_n^N(x)$ vanish for all $n = 0, 1, \dots, M$, $x \in [-1, 1]$. However, suitable expansion coefficients can be obtained by making

the residual functions indicated in Eq.(1.5) small in some sense. Let the inner product of two real-valued functions $\hat{g}_1(t)$ and $\hat{g}_2(t)$ be defined as

$$\langle \hat{g}_1, \hat{g}_2 \rangle_{w_k} = \int_{s=-1}^1 w_k(s) \hat{g}_1(s) \hat{g}_2(s) ds, \quad (1.7a)$$

and the corresponding norm as

$$\|\hat{g}_1\|_{w_k} = \left[\int_{s=-1}^1 w_k(s) \hat{g}_1^2(s) ds \right]^{\frac{1}{2}}, \quad (1.7b)$$

where $w_k(s)$ is a non-negative, real and integrable weight function.

For the collocation method, the orthogonality relation becomes

$$\langle R_n^N(x), \delta(x - x_k) \rangle_1 = 0, \quad n = 0, 1, \dots, M, \quad k = 0, 1, \dots, N. \quad (1.8a)$$

Here, the Dirac delta function is denoted by δ while the $N + 1$ collocation points are indicated as x_k , $k = 0, 1, \dots, N$ and can be defined by the closed rule [12]

$$x_k = \cos\left(\frac{\pi k}{N}\right), \quad k = 0, 1, \dots, N. \quad (1.8b)$$

By choosing this set of $N + 1$ collocation points, the residual functions at the endpoints of the physical domain become zero. This is important since key physical properties are obtained from the endpoints. Note that from Eq. (1.8b), one interprets that $x_0 = 1$ and $x_N = -1$. Error and convergence analyses have been performed illustrating the merit of this choice of basis functions and collocation points in the study of the radiative equation of transfer in both an isotropically [2] and a linear anisotropically scattering medium [3].

Applying the orthogonality condition displayed by Eq. (1.8a) to Eq. (1.5) for $k = 0, 1, \dots, N$ produces

$$\sum_{i=0}^N b_{n,i}^N T_i(x_k) - \frac{\lambda\omega}{2} \sum_{m=0}^M a_m \sum_{i=0}^N b_{m,i}^N \sum_{j=0}^{\tilde{N}_{mn}-1} c_j^{(m,n)} I_{j+1,i}^{(m,n)}(x_k) = \bar{F}_n(x_k), \quad (1.9)$$

$$k = 0, 1, \dots, N, \quad n = 0, 1, \dots, M.$$

This linear system of $(M+1)(N+1)$ equations for the unknown expansion coefficients $b_{n,i}^N$, $n = 0, 1, \dots, M$, $i = 0, 1, \dots, N$ can be solved by matrix inversion. Reconstruction of $\bar{G}_n^N(x)$ can be accomplished with the aid of the expansion shown in Eq. (1.4). Key physical properties can be deduced from the accurate knowledge of the zeroth and first moments.

1.4 Results and Discussion

Numerical results are now presented to illustrate the accuracy of the symbolically enhanced methodology. It is evident that the slab situation described here is of limited utility.

However, extension of such a methodology to spherical problems now appears feasible. All of the numerical results presented in this report were developed using *Mathematica*TM as implemented on a NeXTstation. The entire computer code developed for the general anisotropic scattering case is less than 150 lines in length. This includes the graphical and tabular output statements. Theoretical considerations involving convergence and rigorous error estimates have been performed by Frankel [2] and LaClair and Frankel [3] for the case of isotropic and linear-anisotropic scattering, respectively.

Several "benchmark" problems appear in the thermal radiation literature. It is evident that the present methodology is applicable to the neutron transport equation. The radiation literature is full of benchmark results and thus proof-of-principle is indicated with several well-established radiation problems. For this report, the scope of the presentation is limited to the problem involving uniformly incident radiation of unit intensity at $x = -1$ ($\tau = 0$) and where no radiation is incident at $x = 1$ ($\tau = \tau_d$) [1,4,13,14]. This gives rise to $I^+(-1, \mu) = 1$, and $I^-(1, -\mu) = 0$, $\mu > 0$. Furthermore, let the internal source term, $\bar{s}(x_0)$ be negligible. Therefore, $\bar{F}_n(x)$ reduces to

$$\bar{F}_n(x) = 2\pi \int_{\mu=0}^1 P_n(\mu) e^{\frac{-\lambda(1+x)}{\mu}} d\mu, \quad x \in [-1, 1], \quad n = 0, 1, \dots, M, \quad (1.10a)$$

or upon making a similar observation as noted in developing the kernel functions,

$$\bar{F}_n(x) = 2\pi \sum_{j=0}^{\bar{N}_{0,n}-1} c_j^{(0,n)} E_{j+2}(\lambda(1+x)), \quad x \in [-1, 1], \quad n = 0, 1, \dots, M. \quad (1.10b)$$

Next, consider the two scattering phase functions shown in Figure 2, where the phase coefficients are presented in Table 1. Figure 2a displays a weakly, back-scattering phase function while Fig. 2b portrays a weakly, forward-scattering phase function. Both of these cases are well documented and thus serve as the benchmark cases for consideration.

Using PF1 (backward-scattering case), Table 2 presents numerical results for the reflectivity and transmissivity, as defined by [1,4]

$$R = 1 - \frac{\bar{G}_1(-1)}{\pi} \approx 1 - \frac{\bar{G}_1^N(-1)}{\pi}, \quad (1.11a)$$

and

$$T = \frac{\bar{G}_1(1)}{\pi} \approx \frac{\bar{G}_1^N(1)}{\pi}, \quad (1.11b)$$

respectively, for various optical depths, τ_d and single-scattering albedos, ω . This table also contains the results of three previous investigations. The results of Frankel [1], Thynell and Ozisik [4], and Cengel and Ozisik [13] are presented. Frankel [1] used singularity subtraction and trapezoidal integration to obtain numerical solutions. Thynell and Ozisik [4] developed an intricate solution based on eigenfunction expansions. This methodology required a separate analysis for the conservative case where $\omega = 1$. No special treatment

is required by the present approach when $\omega = 1$. Finally, Cengel and Ozisik [13] developed a Galerkin solution in which Legendre polynomials of the first kind were used in the series representations. It is evident that the present scheme rapidly converges to the "numerically exact" solution offered by Cengel and Ozisik. Upon closer inspection, the present approach appears to be converging faster than the solution developed by Thynell and Ozisik [13].

Using PF2 (forward-scattering case), Table 3 compares the results of Frankel [1], and Menguc and Viskanta [14] to the present approach. It is evident from viewing this table that the flux results, defined as $Q(x) = \bar{G}_1^N(x)$, produced by the present method is comparable to the F-N solution when $\tau_d = 1$ and $\omega = 0.8$.

Symbolic manipulators are commonly considered to be RAM intensive. Figure 3 illustrates the memory requirements for a complete simulation as a function of the approximation order N for PF1 when $M = 5$, $\omega = 0.9$, and $\tau_d = 1$. Memory demands remain minimal and appear to grow linearly with increasing values of N . A plot of the RAM requirements as a function of the degree of anisotropy, M , for fixed N reveals a similar trend. Actual run times for generating numerical solutions using a symbolic manipulator can become excessive as M and N grow. The majority of the CPU time used in a simulation arises from constructing the coefficient matrix and known vector indicated in Eq. (1.9). This situation can be remedied by developing a hybrid method that uses a high-level language for the actual evaluations of $T_i(x_k)$, $I_{j+1,i}^{(m,n)}(x_k)$ and $\bar{F}_n(x_k)$. CPU times then become minimal owing to the nature of the programming language. Combining symbolic manipulation with a high-level language would make such problems routine. Contemporary symbolic packages, such as *Mathematica*TM, allow for this type of interaction.

In concluding this portion of the report, it appears that the symbolically augmented methodology used in concert with orthogonal collocation having a Chebyshev basis set performs well for anisotropically scattering phenomena. Interfacing the present approach with a high-level language reduces the actual computational times.

Acknowledgements: The author also wishes to thank the effort of the two undergraduate students (Mr. Joel Adcock and Ms. Leslie Walls) who assisted in the preparation of the computer code.

1.5 References

- ¹ Frankel, J.I., "Computational Attributes of the Integral Form of the Equation of Transfer," *Journal of Quantitative Spectroscopy and Radiative Transfer*, Vol. 58, # 4, 1991, pp. 329-342.
- ² Frankel, J.I., "Several Symbolic Augmented Chebyshev Expansions for Solving the Equation of Radiative Transfer," *Journal of Computational Physics*, Vol. 117, 1995, pp. 350-363.

- ³ LaClair, T., and Frankel, J.I., "Chebyshev Series Solution for Radiative Transport in a Medium with a Linearly Anisotropic Scattering Phase Function," *Int. J. Numerical Method for Heat and Fluid Flow*, Vol. 5 # 8, 1995, pp. 685-704.
- ⁴ Thynell, S.T., and Ozisik, M.N., "Use of Eigenfunctions for Solving Radiation Transfer in Anisotropically Scattering, Plane-Parallel Media," *J. Applied Physics*, Vol. 60, # 2, 1986, pp. 541-551.
- ⁵ Siegel, R. and Howell, J.R., *Thermal Radiation Heat Transfer*, 3rd ed., Hemisphere Publishing Corp., Washington, 1992.
- ⁶ Wolfram, S., *Mathematica*, 2nd ed., Addison-Wesley, Reading, MA, 1992.
- ⁷ Rivlin, T.J., *The Chebyshev Polynomials*, Wiley, New York, 1974.
- ⁸ Orszag, S., "Accurate Solution of the Orr-Sommerfeld Stability Equation," *J. Fluid Mechanics*, Vol. 50, 1971, pp. 689-703.
- ⁹ Kaya, A.C., and Erdogan, F., "On the Solution of Integral Equations with Strongly Singular Kernels," *Quarterly Applied Mathematics*, Vol. 45, #1, 1987, pp. 105-122.
- ¹⁰ Frankel, J.I., "Cumulative Variable Formulation to Transient Conductive and Radiative Transport in Participating Media," *AIAA J. Thermophys. Heat Transf.*, Vol. 9, #2, 1995, pp. 210-218.
- ¹¹ Frankel, J.I., "A Galerkin Solution to a Regularized Cauchy Singular Integro-Differential Equation," *Quarterly of Applied Mathematics*, Vol. 53, #2, 1995, pp. 245-258.
- ¹² Delves, L.M., and Mohamad, J.L., *Computational Methods for Integral Equations*, Cambridge University Press, Cambridge, 1988.
- ¹³ Cengel, Y.A., and Ozisik, M.N., "The Use of the Galerkin Method for Radiation Transfer in an Anisotropically Scattering Slab with Reflecting Boundaries," *Journal of Quantitative Spectroscopy and Radiative Transfer*, Vol. 32, # 3, 1984, pp. 225-233.
- ¹⁴ Menguc, M.P., and Viskanta, R., "Comparison of Radiative Transfer Approximations for Highly Forward Scattering Planar Medium," *Journal of Quantitative Spectroscopy and Radiative Transfer*, Vol. 29, # 5, 1983, pp. 381-394.

1.6 List of Tables

Table 1: Phase function coefficients denoted as PF1 (backward) and PF2 (forward) corresponding to Figure 2.

Table 2: Comparison of results for the reflectivity, R and transmissivity, T among recent studies using PF1 for various single-scattering albedos, ω and optical depths, τ_d .

Table 3: Comparison of results for the surface heat fluxes among recent studies using PF2 when $\omega = 0.8$ and $\tau_d = 1$.

Term, m	Phase Function 1 (PF1, M=5) Back Scattering Coefficients	Phase Function 2 (PF2, M=6) Forward Scattering Coefficients
0	1	1
1	-0.56524	0.643833
2	0.29783	0.554231
3	0.08571	0.103545
4	0.01003	0.010498
5	0.00063	0.000563
6	—	0.000019

Table 1: Phase function coefficients denoted as PF1 (backward) and PF2 (forward) corresponding to Figure 2.

ω	N	$\tau_d = 0.1$		$\tau_d = 1$		$\tau_d = 5$	
		R	T	R	T	R	T
0.1	4	0.0083562	0.838491	0.0250434	0.229076	0.0287262	0.0019101
	6	0.0083560	0.838491	0.0249877	0.229064	0.0266237	0.0019845
	8			0.0249822	0.229063	0.0263159	0.0019696
	10					0.0262535	0.0019656
	12					0.0262365	0.0019645
	100 Panels [1]	0.0083562	0.838491	0.0249929	0.229064	0.0264040	0.0019642
	N=15 [4]	0.0083545	0.83849	0.024982	0.22906	0.026227	0.0019640
	"Exact" [13]	0.008356	0.838491	0.024981	0.229063	0.026226	0.001964
0.9	4	0.084895	0.895490	0.388626	0.439743	0.513838	0.0486162
	6	0.0848944	0.895490	0.388459	0.439786	0.507288	0.0417609
	8			0.388442	0.439791	0.506409	0.041738
	10					0.506237	0.0417341
	12					0.506189	0.0417334
	100 Panels [1]	0.0848961	0.895490	0.388541	0.439800	0.508286	0.0417555
	N=15 [4]	0.084873	0.89552	0.38847	0.43970	0.50616	0.041720
	"Exact" [13]	0.084895	0.895489	0.388437	0.439792	0.506157	0.041733
1	4	0.0959217	0.904078	0.486903	0.513097	0.821002	0.178998
	6	0.0959213	0.904079	0.486801	0.513199	0.819225	0.180775
	8			0.486791	0.513209	0.819001	0.180999
	10					0.818955	0.181045
	12					0.818943	0.181057
	100 Panels [1]	0.0959232	0.904078	0.486896	0.513217	0.821180	0.181071
	N=15 [4]	0.095890	0.90411	0.48688	0.51312	0.81898	0.18102
	"Exact" [13]	0.095922	0.904078	0.486788	0.513212	0.818934	0.181066

Table 2: Comparison of results for the reflectivity, R and transmissivity, T among recent studies using PF1 for various single-scattering albedos, ω and optical depths, τ_d .

<u>Method</u>		<u>Q(-1)</u>	<u>Q(1)</u>
<i>Present Approach:</i>	N=4	0.760344	0.455868
	N=6	0.760548	0.455877
	N=8	0.760568	0.455879
	N=10	0.760573	0.455879
<i>Frankel</i> [1]	Panels= 40	0.7601053	0.4559390
	Panels= 80	0.7604430	0.4558964
	Panels=100	0.7604881	0.4558906
<i>F-N Method</i> [14]	N=3	0.76061	0.45596
	N=5	0.76058	0.45588
	N=9	0.76057	0.45588

Table 3: Comparison of results for the surface heat fluxes among recent studies using PF2 when $\omega = 0.8$ and $\tau_d = 1$.

1.7 List of Figures

Figure 1: *Mathematica*TM input/output cell displaying the construction of the coefficients $c_j^{(m,n)}$.

Figure 2: Anisotropic scattering phase functions denoted as (a) PF1-weakly, back-scattering ($M = 5$); and, (b) PF2-weakly, forward-scattering ($M = 6$).

Figure 3: Memory requirements as a function of N for fixed $M = 5$.

(*Symbolic determination of coefficients needed for Eq. (2) when the degree of anisotropy, M is specified. The variable "alist" contains each of the desired coefficients in ascending order, j=0,1,..., maxcoeff[m,n]-1, for a given (m,n). Example: Rayleigh scatter, M=2 *)

```
Clear[u,m,n,fmn,coeffc,maxcoeffc,M]
M=2;
arrayc=Array[coeffc,{{(M+1)^2,M+1,M+1},0},0];
arraymaxc=Array[maxcoeffc,{M+1,M+1},0];
Do[Do[
  Clear[alist];
  fmn=Expand[LegendreP[m,u]*LegendreP[n,u],u];
  alist=CoefficientList[fmn,u];
  Print["alist [m = ",m," ,n = ",n," ] = ",alist];
  maxcoeffc[m,n]=Length[alist];
  Do[coeffc[j,m,n]=Part[alist,j+1],
    {j,0,maxcoeffc[m,n]-1}],{m,0,M}],{n,0,M}]

alist [m = 0,n = 0 ] = {1}
alist [m = 1,n = 0 ] = {0, 1}
alist [m = 2,n = 0 ] = {-(-), 0, -}
alist [m = 0,n = 1 ] = {0, 1}
alist [m = 1,n = 1 ] = {0, 0, 1}
alist [m = 2,n = 1 ] = {0, -(-), 0, -}
alist [m = 0,n = 2 ] = {-(-), 0, -}
alist [m = 1,n = 2 ] = {0, -(-), 0, -}
alist [m = 2,n = 2 ] = {-, 0, -(-), 0, -}
```

Figure 1: MathematicaTM input/output cell displaying the construction of the coefficients $c_j^{(m,n)}$.

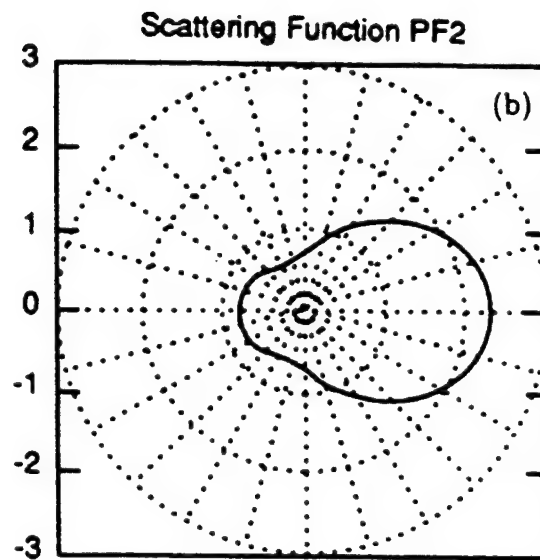
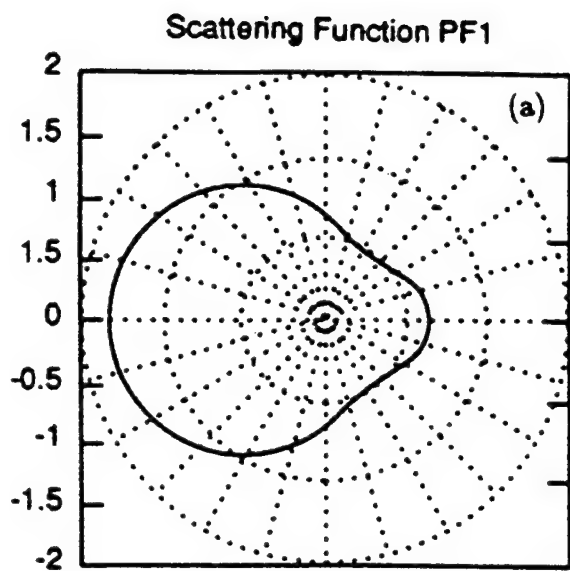
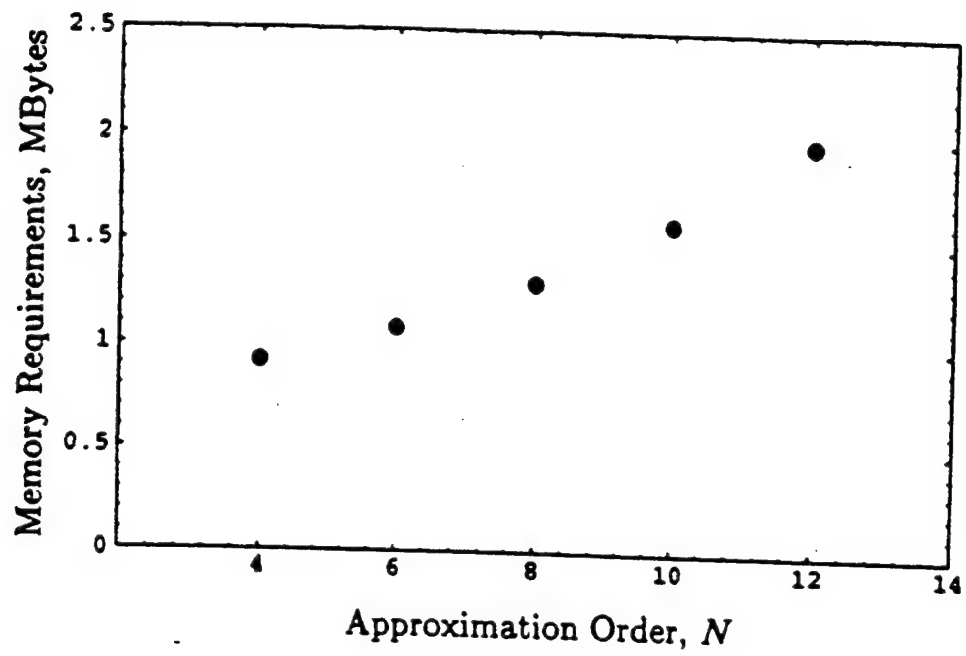


Figure 2: Anisotropic scattering phase functions denoted as (a) PF1-weakly, back-scattering ($M = 5$); and, (b) PF2-weakly, forward-scattering ($M = 6$).



e 3: Memory requirements as a function of N for fixed $M = 5$.

2.0 Task II: Spherical Coordinate Formulation

This portion of the final report addresses Task II as reported in the SOW and described in the Report Organization.

2.1 Introduction

The development of the integral form of the Boltzmann transport equation in the spherical coordinate system is sought since the proposed computational methodology takes advantage of a reduction in dimensionality associated with the integral formalism. It is interesting to note that researchers from both the neutron and radiative transport arenas have considered the integral formalism. However, in general, the communities have consistently addressed the development of numerical methods for solving the conventional integro-differential form of the transport equation.

A brief overview of the pertinent literature is now offered from which an appropriate integral formalism is presented for highly anisotropic scatter in a one-speed situation. The radiative [1-11] and neutron [12-15] communities have considered spherical shell geometries in numerous past studies. Most situations have considered highly idealized scattering situations mainly involving isotropic scattering. Thynell and Ozisik [8] also considered, in the context of radiative transport, the situation where the single-scattering albedo was spatially dependent.

Thynell and Ozisik [9], Abulwafa [10], and Pomraning and Siewart [11] derived the integral form of the transport equation in spherical form. Thynell and Ozisik [9] developed an integral formalism for a solid sphere while Abulwafa [10] developed an integral formalism based on a spherical shell. It is interesting to note that Thynell and Ozisik [9] merely derived the correct system of weakly-singular Fredholm integral equations of the second kind. That is, they did not present any numerical results. Abulwafa [10] presented some numerical results as developed using a Galerkin method based on a monomial set of basis functions. The derivation offered by Abulwafa [10] used a change of variables [15] to arrive at the desired integral formulation. Owing to the general nature of the forms presented by Abulwafa [10] and Thynell and Ozisik [9], it is these forms that appear most satisfactory for the present research program.

2.2 Formulation and Remarks

The conventional integro-differential form of the Boltzmann transport equation in the spherical coordinate system is [9,10,16]

$$\mu \frac{\partial \psi}{\partial r}(r, \mu) + \frac{(1 - \mu^2)}{r} \frac{\partial \psi}{\partial \mu}(r, \mu) + \psi(r, \mu) = Q(r) + \frac{\omega}{2} \sum_{m=0}^M a_m P_m(\mu) \int_{\mu'=-1}^1 P_m(\mu') \psi(r, \mu') d\mu',$$
$$r \in [0, R], \quad \mu \in [-1, 1], \quad (2.1a)$$

where $\psi(r, \mu)$ is the angular flux, ω is the mean number of secondaries per collision, $Q(r)$ represents an isotropic source density function, r is the distance variable measured

in units of mean free path, μ is the cosine of the angle between the propagating flux and the radial coordinate, and R is the radius of the spherical domain of interest. It is not difficult to generalize Eq. (2.1a) further to include a spatially dependent ω , i.e., $\omega \rightarrow \omega(r)$ [9]. The phase function is normally expressed as

$$p(\mu, \mu') = \sum_{m=0}^M a_m P_m(\mu) P_m(\mu'), \quad a_0 = 1, \quad (2.1b)$$

where the coefficients $\{a_m\}_{m=0}^M$ are known and $P_m(\mu)$ represents the m^{th} Legendre polynomial of the first kind. Often incoming distributions are prescribed as boundary conditions at the external surfaces [15,16] in spherical shells. For the solid sphere, we consider the isotropic external condition at $r = R$, namely

$$\psi(R, \mu) = F, \quad \mu = [-1, 1]. \quad (2.1c)$$

Further generalizations on the boundary condition are available.

Following Sahni [15] and Abulwafa [10], we introduce the neutron path coordinates

$$\xi = r\sqrt{1 - \mu^2}, \quad (2.2a)$$

$$\eta = \mu r. \quad (2.2b)$$

Recalling the chain rule from differential calculus, we find

$$\frac{\partial}{\partial r} = \frac{\partial \xi}{\partial r} \frac{\partial}{\partial \xi} + \frac{\partial \eta}{\partial r} \frac{\partial}{\partial \eta}, \quad (2.3a)$$

and

$$\frac{\partial}{\partial \mu} = \frac{\partial \xi}{\partial \mu} \frac{\partial}{\partial \xi} + \frac{\partial \eta}{\partial \mu} \frac{\partial}{\partial \eta}. \quad (2.3b)$$

Introducing Eq. (2.3) into Eq. (2.1a) produces

$$\frac{\partial \Psi}{\partial \eta}(\xi, \eta) + \Psi(\xi, \eta) = \frac{\omega}{2} \sum_{m=0}^N a_m P_m\left(\frac{\eta}{\sqrt{\xi^2 + \eta^2}}\right) G_m(\sqrt{\xi^2 + \eta^2}) + Q(\sqrt{\xi^2 + \eta^2}), \quad (2.4a)$$

where

$$\Psi(\xi, \eta) = \psi(\sqrt{\xi^2 + \eta^2}, \frac{\eta}{\sqrt{\xi^2 + \eta^2}}), \quad (2.4b)$$

and

$$G_m(r) = \int_{\mu=-1}^1 P_m(\mu) \psi(r, \mu) d\mu, \quad m = 0, 1, \dots, N, \quad (2.4c)$$

where we use Abulwafa's definition [10] of $G_m(r)$. (Note that Thynell and Ozisik [9] and Abulwafa [10] have slightly different definitions of the Legendre moments of $\psi(r, \mu)$ in that the factor of 2π is omitted in Abulwafa's definition.) It is evident that $r = \sqrt{\xi^2 + \eta^2}$ and

$\mu = \eta / \sqrt{\xi^2 + \eta^2}$ and that $r \in [0, R]$ and $\mu \in [-1, 1]$ are transformed into $\sqrt{\xi^2 + \eta^2} \in [0, R]$ and $\xi \geq 0$.

At this point, two approaches for arriving at the integral representation can be followed. Thynell and Ozisik [9] considered the forward and backward components separately as was done by Frankel [17] when considering the slab geometry. Abulwafa [10] and Sahni [15] followed a direct route in arriving at the integral form. Using either approach, an integrating factor is introduced and upon a lengthy but relatively straightforward set of manipulations [4], we arrive at a system of weakly-singular Fredholm integral equations of the second kind [10] for the various Legendre moments of $\psi(r, \mu)$, namely

$$rG_n(r) = -FbK_{n1}(r, b) + \int_{y=0}^R y \left[Q(y)K_{n0}(r, y) + \frac{\omega}{2} \sum_{m=0}^N a_m K_{nm}(r, y) G_m(y) \right] dy, \quad n = 0, 1, \dots, N, \quad r \in [0, R], \quad (2.5a)$$

where the kernel $K_{nm}(r, y)$ is given as

$$K_{nm}(r, y) = \int_{t=-|r-y|}^{-(r+y)} P_n\left(\frac{y^2 - r^2 - t^2}{2rt}\right) P_m\left(\frac{y^2 - r^2 + t^2}{2yt}\right) \frac{e^t}{t} dt, \quad (2.5b)$$

The weakly-singular (integrable) nature of these equations are exhibited in the kernel functions. Under certain conditions, the first exponential integral function $E_1(s)$ is produced which contains a known singular point at $s = 0$. Technically, a logarithmic singularity exists at this point. The exponential integral functions $E_k(s)$, $k = 2, 3, \dots$ are nonsingular and thus do not represent any real problems.

For linear anisotropic scattering ($N = 1$), Eq. (2.5a) reduces to

$$rG_0(r) = -FbK_{01}(r, b) + \quad (2.6a)$$

$$\int_{y=0}^R y \left[Q(y)K_{00}(r, y) + \frac{\omega}{2} \left(K_{00}(r, y)G_0(y) + a_1 K_{01}(r, y)G_1(y) \right) \right] dy,$$

and

$$rG_1(r) = -FbK_{11}(r, b) + \quad (2.6b)$$

$$\int_{y=0}^R y \left[Q(y)K_{10}(r, y) + \frac{\omega}{2} \left(K_{10}(r, y)G_0(y) + a_1 K_{11}(r, y)G_1(y) \right) \right] dy, \quad r \in [0, R].$$

For the linear anisotropic case [10], the kernel functions can be identified in terms of exponential integral functions. That is, the kernels expressed in Eq. (2.6a,b) are

$$K_{00}(r, y) = E_1(z) - E_1(x), \quad (2.7a)$$

$$K_{01}(r, y) = [\operatorname{sgn}(r - y)yE_2(z) - E_3(z) + yE_2(x) + E_3(x)]/y, \quad (2.7b)$$

$$K_{10}(\tau, y) = -K_{01}(y, \tau), \quad (2.7c)$$

and

$$K_{11}(\tau, y) = [E_5(x) + ryE_3(x) + xE_4(x) - E_5(z) - zE_4(z) + ryE_3(z)]/(ty), \quad (2.7d)$$

where $z = |r - y|$ and $x = r + y$.

With this observation, the approach developed in Part 1 of this report appears possible. In Phase II of the offered program, it is our intent to generalize the concept put forth in Part 1 of this report to the spherical problem derived in Part 2. Initial consideration will involve using the proposed approach and confirming the results of Abulwafa [10] who has presented benchmark data for the spherical problem. Extension to highly anisotropic scattering will then be considered.

2.3 References

- ¹ Crosbie, A.L., and Khalil, H.K., "Radiative Transfer in a Gray Isothermal Spherical Layer," *J. Quant. Spectrosc. Radiat. Transfer*, Vol. 12, 1972, pp. 1465-1486.
- ² Viskanta, R., and Crosbie, A.L., "Radiative Transfer through a Spherical Shell of an Absorbing-Emitting Gray Medium," *J. Quant. Spectrosc. Radiat. Transfer*, Vol. 7, 1967, pp. 871-889.
- ³ Tsai, J.R., and Ozisik, M.N., "Radiation in Spherical Symmetry with Anisotropic Scattering and Variable Properties," *J. Quant. Spectrosc. Radiat. Transfer*, Vol. 42, 1989, pp. 187-199.
- ⁴ Smith, M.G., "An Approximate Solution of the Spherically Symmetric Transport Equation," *Quart. Journ. Mech. and Applied Math.*, Vol. 16, 1963, pp. 239-252.
- ⁵ Siewert, C.E., and Thomas, J.R., Jr., "Radiative Transfer Calculations in Spheres and Cylinders," *J. Quant. Spectrosc. Radiat. Transfer*, Vol. 34, 1985, pp. 59-64.
- ⁶ Kisomi, A., and Sutton, W.H., "Source Expansion Solutions for Radiative Transfer in Slab, Spherical and Cylindrical Geometries," *J. Thermophys. and Heat Transfer*, Vol. 2, 1988, pp. 370-373.
- ⁷ Tong, T.W., and Swathi, P.S., "Radiative Heat Transfer in Emitting-Absorbing-Scattering Spherical Media," *J. Thermophys. and Heat Transfer*, Vol. 1, 1987, pp. 162-170.
- ⁸ Thynell, S.T., and Ozisik, M.N., "Radiation Transfer in an Isotropically Scattering Solid with Space Dependent Albedo, $\omega(\tau)$," *J. Heat Transfer*, Vol. 107, 1985, pp. 732-734.
- ⁹ Thynell, S.T., and Ozisik, M.N., "The Integral Form of the Equation of Radiative Transfer for an Inhomogeneous, Anisotropically Scattering, Solid Sphere," *IMA Journal of Applied Mathematics*, Vol. 34, 1985, pp. 323-328.

¹⁰ Abulwafa, E.M., "Radiative-Transfer in a Linearly-Anisotropic Spherical Medium," *J. Quant. Spectrosc. Radiat. Transfer*, Vol. 49, 1993, pp. 165-175.

¹¹ Pomraning, G.C., and Siewart, C.E., "On the Integral Form of the Equation of Transfer for a Homogeneous Sphere", *J. Quant. Spectrosc. Radiat. Transfer*, Vol. 28, 1982, pp. 503-506.

¹² Kschwendt, H., "Application of the j_N Method to Neutron Transport in Slabs and Spheres," *Nucl. Sci. Engng.*, Vol. 36, 1969, pp. 447-450.

¹³ Harms, A.A., and Attia, E.A., "Directional Discontinuous Harmonic Solutions of the Neutron Transport Equation in Special Geometry," *Nucl. Sci. Engng.*, 1975, pp. 310-317..

¹⁴ Ganapol, B.D., "Time-Dependent Moments of the Monoenergetic Transport Equation in Spherical and Cylindrical Geometry," *Nucl. Sci. Engng.*, 1976, pp. 103-105.

¹⁵ Sahni, D.C., "Neutron Transport Problems in a Spherical Shell," *J. Math. Phys.*, Vol. 16, 1975, pp. 2260-2270.

¹⁶ Duderstadt, J.J., and Martin, W.R., *Transport Theory*, Wiley, New York, 1979.

¹⁷ Frankel, J.I., "Computational Attributes of the Integral Form of the Equation of Transfer," *Journal of Quantitative Spectroscopy and Radiative Transfer*, Vol. 58, # 4, 1991, pp. 329-342.

DISTRIBUTION LIST

DEPARTMENT OF DEFENSE

DIRECTOR
ARMED FORCES RADIOBIOLOGY RSCH INST
INFORMATION SERVICES DEPT
8901 WISCONSIN AVENUE
BETHESDA, MD 20889-5603

ATTN: MRA
ATTN: PHY, M. WHITNALL
ATTN: TECHNICAL LIBRARY

COMMANDANT
DEFENSE INTELLIGENCE COLLEGE
WASHINGTON, DC 20301-6111
ATTN: DIC/2C
ATTN: DIC/RTS-2

DEFENSE TECHNICAL INFORMATION CENTER
8725 JOHN J KINGMAN RD., SUITE 0944
FORT BELVOIR, VA 22060-6218
ATTN: DTIC/OCF

DEFENSE THREAT REDUCTION AGENCY
6801 TELEGRAPH ROAD
ALEXANDRIA, VA 22310-3398
ATTN: CP
ATTN: CPW, C MCFARLAND
ATTN: CPWCT
ATTN: CPWT
ATTN: NSC
ATTN: NSE

DEFENSE THREAT REDUCTION AGENCY
ALBUQUERQUE OPERATIONS
1680 TEXAS ST. SE
KIRTLAND AFB, NM 87117-5669
ATTN: CPTO
ATTN: TTV 3416TH TTSQ

DIRECTOR
DISA
TECHNICAL RESOURCES CENTER
7010 DEFENSE PENTAGON
WASHINGTON, DC 20301-7010
ATTN: JNGO

PRESIDENT
NATIONAL DEFENSE UNIVERSITY
FORT LESLEY J MCNAIR
WASHINGTON, DC 20319-6000
ATTN: ICAF, TECH LIB

USSTRATCOM/J531T
901 SAC BLVD STE BB11
OFFUTT AFB, NE 68113-5160
ATTN: J-521

DEPARTMENT OF DEFENSE CONTRACTORS

INSTITUTE FOR DEFENSE ANALYSES
1801 N BEAUREGARD STREET
CONTROL & DISTRIBUTION
ALEXANDRIA, VA 22311
ATTN: DOUGLAS SCHULTZ

ITT INDUSTRIES
ITT SYSTEMS CORPORATION
ATTN: AODTRA/DASIAC
1680 TEXAS ST SE
KIRTLAND AFB, NM 87117-5669
ATTN: DASIAC
ATTN: DASIAC/DARE

SCIENCE APPLICATIONS INTL CORP
10260 CAMPUS POINT DRIVE
SAN DIEGO, CA 92121-1578
ATTN: D KAUL, MS 33
ATTN: E SWICK, MS 33
ATTN: L HUNT
ATTN: R J BEYSTER, M/S 47
ATTN: W WOOLSON

SCIENCE APPLICATIONS INTL CORP
P O BOX 1303
MCLEAN, VA 22102
ATTN: J MCGAHAN
ATTN: J PETERS
ATTN: P VERSTEEGEN

UNIVERSITY OF TENNESSEE - KNOXVILLE
COLLEGE OF ENGINEERING
414 DOUGHERTY ENGINEERING BUILDING
KNOXVILLE, TN 37996-2210
ATTN: JAY I FRANKEL

DEPARTMENT OF ENERGY

DEPARTMENT OF ENERGY
OAK RIDGE NATIONAL LABORATORY
X-10 LABORATORY RECORDS DEPT.
P O BOX 2008
OAK RIDGE, TN 37831-6363
ATTN: G KERR, MS 6480
ATTN: J JOHNSON
ATTN: J PACE, MS 6363
ATTN: J WHITE/MS 6362

DEPARTMENT OF THE AIR FORCE

AIR UNIVERSITY
BLDG 1405 ROOM 160 DOCUMENT CONTROL
MAXWELL AFB, AL 36112
ATTN: STRATEGIC STUDIES

AIR UNIVERSITY LIBRARY
600 CHENNAULT CIRCLE
BLDG 1405 - ROOM 160
MAXWELL AFB, AL 36112-6424
ATTN: AUL-LSE
ATTN: LIBRARY

DIRECTORATE OF NUCLEAR
AND COUNTERPROLIFERATION
DEPARTMENT OF THE AIR FORCE
WASHINGTON, DC 20330
ATTN: XOSS

HQ 497 IG/INOT
5113 LEESBURG PIKE
SUITE 600
FALLS CHURCH, VA 22041-3230
ATTN: INT

NATIONAL AIR INTELLIGENCE CENTER
4180 WATSON WAY
WRIGHT-PATTERSON AFB, OH 45433-5648
ATTN: NAIC/GTA

DEPARTMENT OF THE ARMY

COMMANDER
NUCLEAR EFFECTS DIVISION
DEPARTMENT OF THE ARMY
WHITE SANDS MISSILE RANGE, NM 88002-5176
ATTN: STEWS-NE-T

COMMANDER
US ARMY COMBAT SYSTEMS TEST ACTIVITY
ABERDEEN PROVING GROUND, MD 21005-5059
ATTN: C HEIMBACH
ATTN: JOHN GERDES/CSTA-RSAD/BLG 860
ATTN: MIKE STANKA

US ARMY CONCEPTS ANALYSIS AGENCY
ATTN: CSCA-EN
8120 WOODMONT AVENUE
BETHESDA, MD 20814-2797
ATTN: TECHNICAL LIBRARY

US ARMY MODEL IMPROVEMENT STUDY
MANAGEMENT AGENCY
SUITE 808 CRYSTAL SQUARE 2
1725 JEFFERSON DAVIS HIGHWAY
ARLINGTON, VA 22202
ATTN: (SFUS-MIS)

US ARMY NATIONAL GROUND INTELLIGENCE
CENTER
220 7TH STREET, NE
CHARLOTTESVILLE, VA 22901-5396
ATTN: C WARD (IANGIC-RMT)

COMMANDER
US ARMY NUCLEAR & CHEMICAL AGENCY
7150 HELLER LOOP
SUITE 101
SPRINGFIELD, VA 22150-3198
ATTN: MONA-NU (CPT UMEND)

DIRECTOR
US ARMY VULNERABILITY/LETHALITY
ASSESSMENT MANAGEMENT OFFICE
ABERDEEN PROVING GROUND, MD 21005-5001
ATTN: AMSLC-VL-NE (DR J FEENEY)